Isolation, Identification and Characterization of Plastic Degrading Gut Bacteria from *Zophobas atratus* Larvae

By

Ifthikhar Zaman
23376006

A thesis submitted to the Department of Mathematics and Natural Sciences in partial fulfillment of the requirements for the degree of
Master of Science in Biotechnology

Department of Mathematics and Natural Sciences
Brac University
April, 2024

Declaration

It is hereby declared that

1. The thesis submitted is my original work while completing my degree at Brac University.
2. The thesis does not contain material previously published or written by a third party, except where this is appropriately cited through full and accurate referencing.
3. The thesis does not contain material that has been accepted, or submitted, for any other degree or diploma at a university or other institution.
4. I have acknowledged all main sources of help.

Student's Full Name & Signature:

Ifthikhar Zaman
23376006

Approval

The thesis titled "Isolation, Identification and Characterization of Plastic Degrading Gut Bacteria from *Zophobas atratus* Larvae" submitted by

1. Ifthikhar Zaman (23376006)

of Spring, 2024 has been accepted as satisfactory in partial fulfillment of the requirement for the degree of MS in Biotechnology on [Date-of-Defense].

Examining Committee:

Supervisor:
(Member)

Dr. M. Mahboob Hossain
Professor, Microbiology Program,
Department of Mathematics and Natural Sciences
Brac University

Program Director:
(Member)

Dr. Munima Haque
Associate Professor, Biotechnology Program,
Department of Mathematics and Natural Sciences
Brac University

External Expert Examiner:
(Member)

Dr. MD. Latiful Bari
Chief Scientist, Centre for Advanced Research in Sciences
(CARS)

Departmental Head:
(Chair)

A F M Yusuf Haider, PhD
Professor, Department of Mathematics and Natural Sciences
Brac University

Ethics Statement

This research is done under proper supervision and it is the author's original work. No animal was harmed during experiments. The article is written in a manner that the write-up does not contain material previously published or written by a third party, except where this is appropriately cited through full and accurate referencing. The experiment was done by maintaining all the rules and regulations of the Biotechnology and Microbiology laboratory of the Department of Mathematics and Natural Sciences, BRAC University.

Abstract

Plastic pollution has become a major environmental concern globally, and novel and eco-friendly approaches like bioremediation are essential to mitigate the impact. This study investigated the biodegradation of three common plastic types, LDPE, LLDPE, and EPS, by *Zophobas atratus* larvae. Over 36 days, the average larval consumption was found to be 24.04% LDPE, 20.01% EPS and 15.12% LLDPE. FTIR analysis confirmed plastic oxidation in the gut. Gut bacteria were selectively isolated and identified as *Pseudomonas aeruginosa* strains. These bacteria showed the ability to degrade specific plastic types confirmed by SEM. Whole genome sequencing revealed many enzymes, along with virulence factors, antibiotic-resistance genes, and rhamnolipid biosurfactant biosynthesis genes in both isolates. Rhamnolipid analysis and AST were performed. This study indicated *Zophobas atratus* larvae as potential LDPE, LLDPE, and EPS biodegradation agents. Additionally, the isolated strains of *Pseudomonas aeruginosa* provide a more direct and eco-friendly solution for plastic degradation.

Keywords: *Zophobas atratus*; Linear low-density polyethylene; Low-density polyethylene; Expanded polystyrene; Biodegradation; *Pseudomonas aeruginosa*

Dedication

I dedicate this Thesis work to my family.

Acknowledgment

I am very much thankful to certain people for supporting me in this journey. First, I want to congratulate myself for completing the thesis successfully by abiding by the rules as much as possible. I am thankful to my parents, who have never stopped supporting me and were beside me in every moment of my life. I am very humbly indebted to my thesis supervisor, Professor Dr. M. Mahboob Hossain, Department of Mathematics and Natural Sciences, who guided me efficiently in this journey and without whom, the research would not be possible and helped me to find my true potential as a researcher. I would like to thank Professor Dr. A F M Yusuf Haider, Chairperson, MNS department for allowing me to do research on this topic. I am also thankful to Dr. Munima Haque, Associate Professor, MNS department for her helpful advices. I would like to thank Professor Dr. Aparna Islam, MNS department for motivating and supporting me throughout the journey. I would like to thank some of my lab colleagues, Shabnoor Binte Dayem, Research Assistant; Tamanna Islam Toma, Research Assistant; Nazifa Tabassum Tasnim, Research Assistant for having my back and supporting me. I would like to thank Rafeed Rahman Turjya, former lecturer, Brac University; Md Salman Shakil, lecturer, Brac University; Akash Ahmed; senior lecturer, Brac University for their support. I am also thankful to Mahruf Al Shahariar and Rezanur Rahman Howlader. I would like to also thank the lab assistants who made the lab work so much easier. I would like to show my gratitude to Dr. Muntasir Alam, Assistant Scientist, Emerging Infections, Infectious Diseases Division, icddr,b, and Afsana Rashed, Research Assistant, Infectious Disease Division, icddr,b for prompt response to my samples and sequencing.

Table of Contents

List of Tables

List of Figures

List of Acronyms

LDPE	Low-Density Polyethylene
EPS	Expanded Polystyrene
LLDPE	Linear Low-Density Polyethylene
SEM	Scanning Electron Microscopy
FTIR	Fourier Transform Infrared Spectroscopy

Chapter 1

Introduction

1.1 Bioremediation

Bioremediation, an environmentally friendly and advanced technique, utilizes natural biological processes to eliminate harmful contaminants from the environment, as defined by (Vidali, 2001). The escalating concern over environmental pollution worldwide is largely attributed to increased fossil fuel production and consumption (Omokhagbor Adams et al., 2020). In light of this pollution crisis, bioremediation emerges as a pivotal solution, leveraging microbes, fungi, insects, and green plants instead of chemical substances to restore environmental integrity. Bioremediation encompasses two main approaches: in-situ and ex-situ. In-situ bioremediation treats pollutants directly at the site of contamination without excavation, offering cost-effective advantages over ex-situ methods. Addressing the urgent need for environmental sustainability requires embracing green technologies like bioremediation to remediate polluted ecosystems affected by human activities, industrialization, and agricultural practices (Arora, 2018; Juwarkar et al., 2010). Bioremediation, however, faces challenges, including the specific selection of microorganisms, the potential toxicity of biodegradation by-products, and slower kinetics compared to conventional methods (Abatenh et al., 2017). Despite these drawbacks, bioremediation holds promise as an effective and eco-friendly solution, necessitating further research to comprehend microbial degradation processes (Chatterjee et al., 2008). With its minimal environmental impact and suitability for deployment in contaminated areas, bioremediation stands as a vital technology in achieving sustainable development and mitigating global climate challenges.

1.2 Plastics

The term "plastic" is derived from the Greek word "plastikos," meaning "capable of being molded into various shapes." Plastics are comprised of carbon, hydrogen, silicon, oxygen, chloride, and nitrogen, and are primarily sourced from oil, coal, and natural gas. Polyethylene, a linear hydrocarbon polymer formed by long chains of ethylene monomers (C_2H_4), constitutes approximately two-thirds, or precisely 64%, of all plastic (Goosey, 1985). Plastics play an indispensable role in the global economy, finding extensive application in agriculture, construction, healthcare, and various other sectors. They serve as the cornerstone of numerous industries due to their versatility in manufacturing a wide array of products, ranging from household items to defense components. Additionally, plastics are utilized in the packaging of cosmetics, detergents, and pharmaceuticals. However, the excessive use of plastics poses a significant threat to both the environment and human well-being. The accumulation of plastics on land and in oceans has spurred considerable interest in the degradation of these polymers. To mitigate the adverse environmental effects of plastics, biodegradation methods are imperative. Understanding the interaction between microbes and polymers is critical in addressing plastic-related challenges. Many organisms, predominantly bacteria, have evolved strategies for the survival and decomposition of plastics (Oliveira et al., 2020). This study was focused on three different types of plastics, including Low-Density Polyethylene (LDPE), Expanded Polystyrene (EPS), and linear Low-Density Polyethylene (LLDPE).

1.3 Bioremediation of Plastics

Non-biodegradable plastics persist for centuries, ultimately transforming into contaminating microplastics that reenter food chains (Chamas et al., 2020). Their presence has become widespread in our air, water, soil, and food items (Wright et al., 2021). In 2017, global plastic emissions amounted to 0.8 million tons (mt) of microplastics and 8.7 mt of macroplastics; by 2050, this emission may increase to 2.2 gigatonnes (Gt) and 3.1 Gt respectively (Schwarz et al., 2023). These findings indicate the severity of plastic pollution and necessitate the development of safe, rapid, and effective plastic remediation methods. With this in mind, there is a wide range of commercially available plastics with different utilities, such as polyethylene (PE) - which can be of high, low, linear density, expanded polystyrene (EPS), polyethylene terephthalate (PET), polyvinyl chloride (PVC), and polypropylene (PP), etc. (Landrock, 1995). Among them, linear low-density polyethylene (LLDPE), low-density polyethylene (LDPE), and expanded polystyrene (EPS) are three of the most used plastic types in the world (Chamas et al., 2020). PE is a type of polyolefin that has a chemical formula of $(C_2H_4)_n$, which is a polymer of ethylene (or ethene) monomer produced by addition or radical polymerization by Ziegler-Natta polymerization or metallocene catalysis methods (Landrock, 1995). In this study, two types of PE were used, LDPE and LLDPE. LDPE is a type of branched PE, which has a high degree of short-chain branching along with long-chain branching with a density of 0.917-0.940 g/cm^3. It has low crystallinity, is highly amorphous, and has very low water absorption capability (Landrock, 1995). On the other hand, LLDPE is a linear polymer with significant numbers of short branches with a density of 0.915-0.950 g/cm^3. Both LDPE and LLDPE are used to manufacture grocery bags, garbage bags, packaging film, agricultural mulch, insulation for wires and cables, bottles, toys, housewares, etc. Similarly, EPS is a white foam plastic material produced from solid beads of polystyrene with the chemical formula $(C_8H_8)_n$ and a

density of 0.012-0.05 g/cm^3 (Landrock, 1995). It is used in foam packaging, CD and DVD cases, insulation, peanuts for shipping, food packaging, meat/poultry trays, and egg cartons.

Plastic pollution has become a global problem due to inadequate recycling compared to its widespread use. Currently, chemical methods and bioremediation are used for remediating environmental plastics. Unfortunately, chemical remediation methods have some negative effects on the environment. On the other hand, bioremediation processes use microorganisms like bacteria, fungi, algae or insects to degrade, remove, change, immobilize, or detoxify pollutants from the environment, which is an eco-friendly alternative (Omokhagbor Adams et al., 2020)**.** Characteristics of the targeted plastics like mobility, crystalline structure, molecular weight, functional groups and additives, etc. influence the effectiveness of bioremediation. To undergo the process, microorganisms need to adhere to the surface of the plastics, followed by colonization, conversion of polymers to monomers, and finally monomers to simple compounds like CO_2, water, ethylene glycol, etc. (Shah et al., 2008). Enzymatic degradation is one of the main mechanisms of these conversions when hydrolytic enzymes such as cutinase, lipase, proteinase K, dehydrogenase, etc. perform hydrolysis (Mohee and Unmar, 2007)**.**

Multiple studies have aimed to find suitable microorganisms to degrade different types of plastics. For example, *Brevibacillus borstelensis* and *Rhodococuus ruber* were identified as potential LLDPE-degrading microorganisms (Hadad et al., 2005; (Orr) et al., 2004). Moreover, PS-degrading bacteria like *Acinetobacter* sp. (Wang et al., 2020), *Serratia marcescens*, *Pseudomonas* sp., *Bacillus* sp. (Galgali et al., 2002), and LDPE-degrading bacteria like *Pseudomonas* sp. (Rajandas et al., 2012; Tribedi and Sil, 2013), *Bacillus amyloliquefaciens* (Nowak et al., 2011) have been isolated. In the meantime, other enzymes have also been identified that facilitate plastic degradation, such as alkane monooxygenase, laccase, and alkane hydroxylase (Bardají et al., 2019; Kim et al., 2021a; Santo et al., 2013).

Insects can also be used for plastic degradation. Since there is limited necessity to pre-condition plastics, it is possible to save time and money. Insects can act on their own and adapt to the changes in the environment. Moreover, they break down the plastics during consumption, which helps bacteria to degrade plastic better. Sometimes the gut bacteria gets additional assistance in the degradation from the enzymes secreted by the insects. For this advantage, extensive research is ongoing in this field, as multiple insect species have shown the capacity to degrade plastic. Biodegradation of PS by the larvae of *Tenebrio molitor* Linnaeus (mealworms) was first reported in 2015 (Yang et al., 2015a, 2015b). The same larvae were also observed to perform LDPE biodegradation (Brandon et al., 2018). Another insect larvae, *Galleria mellonella*, also known as greater wax moths, has been shown to degrade LDPE (Bombelli et al., 2017) and PS (Lou et al., 2020). *Galleria mellonella* has two enzymes in their saliva - 'Demetra', an arylphorin, and 'Ceres', a hexamerin - which can degrade PE within a few hours at room temperature (Sanluis-Verdes et al., 2022). Furthermore, *Tenebrio obscurus* (dark mealworm) is also reported to degrade PS (Peng et al., 2019) and LDPE (Yang et al., 2021b). Lastly, *Zophobas atratus* (synonymous with *Z. morio*, Coleoptera: Tenebrionidae) is another well-known insect that can degrade several types of plastics. This insect, also known as "Superworm", is a type of darkling beetle. This species is known to be a good nutrient source for livestock animals and aquaculture (Jabir et al., 2012; Rumbos and Athanassiou, 2021). Previous studies have revealed that at the larval stage, this insect can biodegrade plastics of different types (Sun et al., 2022), such as PS and LDPE (Peng et al., 2020), and polypropylene (Yang et al., 2021a). Most of these studies were done with LDPE and PS, but not with LLDPE (Peng et al., 2020; Yang et al., 2020; Zielińska et al., 2021). Moreover, although there is available data on the plastic-consuming capability of this insect from a few countries, no such data is available for Bangladesh. Interestingly, studies strongly indicate that their gut microbiome is connected with the biodegradation of plastics (Sun et al., 2022; Yang et al.,

2020). Studies show that the gut microbiome associated with plastic degradation includes genera from *Pseudomonas*, *Rhodococcus,* and *Corynebacterium* (Sun et al., 2022). Genomic data is absent for the potential plastic-degrading bacteria that constitute this microbiome.

The focus of this study revolved around the degradation of LDPE, LLDPE, and EPS, as these plastic types are produced commercially and used indiscriminately in Bangladesh. The bioremediation capacity of *Z. atratus* provides a potentially sustainable solution for the widespread effect of these plastics on the environment. Additionally, this study focused predominantly on the *Pseudomonas* genus, as they are known for their ability to survive in xenobiotic environments and their plastic-degrading capabilities (Wilkes & Aristilde, 2017; Wasi *et al.*, 2013; Lee *et al.*, 2020). For the experiments, the plastic degradation capability of the locally cultivated larvae was assessed on LDPE, LLDPE, and EPS samples collected from markets. After feeding on the plastics, consumed plastic and larval frass were analyzed by Fourier Transform Infrared Spectroscopy (FTIR). Potential bacteria were isolated from the frass, and Scanning Electron Microscopy (SEM) was performed to prove the biodegradation of plastic feed. Whole Genome Sequencing was performed on the isolated bacteria followed by annotation. This study aimed to establish the plastic-degrading capability of the larvae at room conditions as well as gather and analyze the genomic data of the insects' gut bacteria which are involved in the degradation**.**

1.4 *Zophobas atratus*

Zophobas atratus, commonly known as the superworm, is renowned for its substantial size, feeding capacity, and both biological and economic potential. Previous studies have highlighted its nutritional value, making it a valuable nutrient and antimicrobial source for

poultry feed. Recent research has also revealed its potential for waste management as a bioremediation agent (Rumbos & Athanassiou, 2021).

Taxonomic classification of *Z. atratus* has been subject to confusion, with recent research suggesting it to be conspecific with *Zophobas morio*, formerly known as *Tenebrio atratus*, and *Zophobas rugipes* (Tschinkel, 1984). *Z. atratus* belongs to the large beetle family Tenebrionidae (Park et al., 2013). Throughout its lifecycle, *Z. atratus* typically undergoes four distinct stages: Eggs, Larvae, Pupa, and Adults (Rumbos & Athanassiou, 2021). Female *Z. atratus* lay a significant number of oval-shaped eggs (approximately 2200) during their lifetime, each measuring around 1.7 mm in length and 0.7 mm in width (Fursov & Cherney, 2018). Larvae are typically cylindrical, about 55 mm long, with a sclerotized exoskeleton and 7 to 9 abdominal segments. The subsequent pupal stage lasts approximately 13-15 days, during which the pupae exhibit primarily quiescent behavior, although they can display defensive responses such as rotating the abdominal portion (Ichikawa & Kurauchi, 2009). Upon completing the pupal stage, *Z. atratus* emerges as an adult with a body length ranging from 38 to 57 mm, characterized by an elongated body and filiform antennae, with an average lifespan of about 180 days (Fursov & Cherney, 2018).

The larvae stage of *Z. atratus* holds significant biological and commercial importance, particularly as animal feed. In certain ethnic groups in Mexico, species of *Zophobas* are consumed as food (Ramos-Elorduy, 2009). In Brazil, *Z. atratus* is considered a potential protein and nutrient source for livestock and aquaculture feed (Soares Araújo et al., 2019). Recent studies have indicated that the plastic degradation capability of *Z. atratus* primarily resides in its gut microbiome, with certain bacterial strains, such as *Pseudomonas*, being isolated for further investigation toward utilizing *Z. atratus* as a potential bioremediation agent (Peng et al., 2020; Y. Yang et al., 2020). When the gut microbiome was treated with antibiotics, the

plastic degradation ability of the superworm was significantly reduced, underscoring the contribution of the gut microbiome to this capability (Peng et al., 2020; Y. Yang et al., 2020).

1.5 Fourier Transform Infrared Spectroscopy (FTIR)

FTIR spectroscopy operates on the principle of interference between two beams of radiation, resulting in the generation of an interferogram. This signal is produced based on changes in path length between the beams reflected from mirrors within the interferometer block. Through Fourier transformation, distance and frequency domains are mathematically interconverted, giving rise to the name Fourier Transform Infrared Spectroscopy.

The key distinction between an FTIR spectrometer and a dispersive IR spectrometer lies in the use of the Michelson interferometer. The Michelson interferometer serves as the central component of FTIR spectrometers, dividing one light beam into two to create distinct paths. Subsequently, it combines the beams before directing them to the detector, where intensity differences between the two beams are measured relative to path variations. Essential components of FTIR include IR sources, detectors, beam splitters, and Fourier transforms. Third-generation FTIR spectrometers offer notable advantages, including significantly improved signal-to-noise ratios compared to earlier generations, rapid scanning of all frequencies (approximately 1 second), and exceptionally high resolution (0.1 ~ 0.005 cm^{-1}). They also boast high accuracy in wave number measurements and a wide scan range (1000 ~ 10 cm^{-1}), along with reduced interference from extraneous light sources.

However, limitations of FTIR spectroscopy include the compact size of the sampling chamber, which restricts the size of samples that can be analyzed. Additionally, obstructive mounted pieces may interfere with the IR beam, further limiting sample size. Certain materials may completely absorb infrared radiation, rendering measurement impossible in such cases (*FTIR*

Micro-Spectrometer - BDD : Industrial Synchrotron Light Research Institute (Public Organization), n.d.)

1.6 Scanning Electron Microscopy (SEM)

The scanning electron microscope (SEM) utilizes electrons, rather than light, to generate images. Since their inception in the early 1950s, SEMs have significantly advanced research across various disciplines in the medical and physical sciences by enabling the examination of a broader range of specimens.

Compared to traditional microscopes, SEMs offer several advantages. They possess a large depth of field, allowing for more of a specimen to remain in focus simultaneously. Additionally, SEMs boast higher resolution capabilities, enabling the magnification of closely spaced specimens at greater levels. Unlike optical lenses, SEMs utilize electromagnets, granting researchers greater control over magnification levels. These advantages, coupled with the production of remarkably clear images, establish the SEM as a highly valuable research instrument.

Operationally, the SEM functions by producing a highly magnified image through the utilization of an electron beam emitted from an electron gun situated at the top of the microscope. This electron beam traverses a vertical path within a vacuum environment contained within the microscope. Along its path, the beam passes through electromagnetic fields and lenses, which focus it toward the specimen. Upon contact with the specimen, electrons and X-rays are emitted. Detectors within the SEM capture these emitted X-rays, backscattered electrons, and secondary electrons, converting them into a signal that is transmitted to a screen akin to a television screen, ultimately producing the final image (*Scanning Electron Microscope - Environmental Health and Safety - Purdue University*, n.d.).

Chapter 2

Materials and Methods

2.1 Working Place for the Study

The present research work was performed in the Biotechnology and Microbiology Laboratory of the Department of Mathematics and Natural Sciences, BRAC University, KHA 224, Progati Sarani, Merul Badda, Dhaka 1212.

2.2 Media, Solutions, and Reagents

Media, reagents, and solutions that were used in this thesis work were available as a reagent grade, and without further purification, those were used.

2.3 Handling of Laboratory Equipment

Detergents were used to wash all the glassware and rinsed 4-5 times with tap water. Autoclavable equipment was sterilized by autoclaving at 121° C for 15 minutes at 15 psi. All the microbiological works were done inside the Biological Safety Cabinet. Larvae were kept in PET boxes which were in a hardboard box and safety was maintained so that no larvae could leave the box.

2.4 Sample collection

About 300 pieces of *Zophobas atratus* larvae were bought from "Green Field Agro", a commercial cultivator from Pallabi, Mirpur, Dhaka, Bangladesh who was breeding the larvae for use as poultry/reptile feed, in a PET box with rice bran to feed them. The larvae were identified based on their morphology and darker color.

2.5 Preparation for Larvae Sample

2.5.1 Plastic Preparation

Three types of plastic were chosen, LDPE, LLDPE, and EPS. These plastics were cut into square or rectangular shapes, measured by weight, and put in three different empty PET boxes. The same process was done for the main process after 14 days.

For bacteriological studies, LDPE, LLDPE, and EPS were cut into 1 x 1 cm size and transferred into a beaker with distilled water and stirred for another 10 minutes. This step was repeated 3 times until all plastics were ridden of any residual surface dust. Then, they were aseptically placed in a 70% ethanol solution for 30 minutes. Finally, the disinfected plastics were transferred to a sterile petri dish dried in the laminar hood, and put away for further use.

2.5.2 Larvae Preparation

At the start of the study, the average weight of the larvae was 388 ± 23 mg. There was confirmation from the cultivators that the larvae had no antibiotics in their system as they were given antibiotic-free feeds. The absence of antibiotics was important, as their use in the feed would inhibit gut bacteria which were explored in this study. The organic feed used in this study was locally sourced rice bran.

2.6 Plastic Biodegradation Rate and Larvae Survivability Analysis

Z. atratus larvae were subjected to plastic consumption tests followed by survivability rate (SR) tests. The larvae were only fed rice bran for 18 days after collection from the cultivator. All the larvae were kept in the same environmental condition with the same rice bran provided as feed. After 18 days, three PET boxes were used to house the larvae, ensuring that no light could penetrate inside. Although PET itself is a type of plastic, *Z. atratus* larvae have not shown PET-degradation capability; hence PET boxes were used in this study. Each box was designated for a different plastic-type, and it was ensured that there was no edible material in the box that the larvae could feed on. The lids of the boxes had small holes for the circulation of air. For each plastic type, about 20 larvae were chosen randomly and put in the designated

box. Then for the next 14 days, the larvae were kept with the plastic as the only food source to clear out the digestive system of any previous organic food. For positive control (PCN), a separate PET box was designated and 20 randomly selected larvae were kept inside with rice bran as a food source. Similarly, for negative control (NCN), another PET box was designated and 20 randomly selected larvae were kept inside with no food source. The frass was removed from the boxes every two days. After 14 days, all the used plastics and frass (rice bran for the PCN) were removed. The larval live average weight was measured for every box at this stage. Then, fresh weighted plastics were introduced according to the box designation (only rice bran for PCN) and data was collected over the next 36 days. The boxes were put in a bigger container which again was ensured to have no light penetration. The experiment was done at room temperature with no commercial incubator. For 36 days, the weight of the plastics was measured every 2 days to determine how much plastic was being eaten by the larvae. It was repeatedly ensured that no outside organic food source was available in the boxes. Additionally, frass was removed every 2 days and average larvae live weight was measured in the meantime. A live larvae count was carried out every day to check how many larvae have survived. Live larvae weight measurement was done every 2 days for the full length of the experiment (36 days) and onwards. However, after the first 15 days, frass was not removed for 7 days so that enough frass could be collected for bacteriological and chemical experiments. Then frass removal was again resumed every 2 days.

Plastic consumption data was calculated as follows:

$$\text{Plastic Consumption (PC) (\%)} = (P_{36}/P_0)*100\%$$

Where P_{36} is the total consumed plastic after 36 days and P_0 is the initial weight of the plastic.

Larvae survivability data was calculated as follows:

$$\text{Survivability Rate (SR) (\%)} = (S_{36}/S_0)*100\%$$

Where S_{36} is the total live larvae remaining after 36 days and S_0 is the initial larvae amount.

Lastly, for larvae average weight was calculated as follows:

$$\text{Larvae Average Weight (LW)} = W_x/N_x$$

Where W is the combined weight of all the larvae in a box at x day, and N is the number of live larvae at x day. All the experiments were done in triplicate and the final result was formed with the average of the triplicate results.

2.7 Frass Bacteria Culture, Isolation, and Identification

By the 22nd day of the experiment, enough frass was accumulated in the PET boxes, so it was collected. Frass collected from the same designated boxes was mixed to prepare three master frass stocks (one each for the different plastic types). From each of the master stocks, 0.1g of frass was mixed in 10 ml 0.9% NaCl solution, and serial dilution was done up to 10^{-4} dilution. After dilution, 2.5 ml of each sample was inoculated in 250 ml of Minimal Salt (MS) broth. The MSB media composition was as follows: KH_2PO_4 (3g/L), K_2HPO_4 (0.1g/L), NaCl (5g/L), NH_4Cl (2g/L), $MgSO_4.7H_20$ (0.16g/L), $CaCl_2.2H_20$ (0.1g/L), with pH adjusted to 7.0 (Fazito do Vale et al., 2007). The media was sterilized by autoclaving at 121°C with 15 psi for 15 minutes. MS broth contained only salt and no carbon source, so plastics as a sole carbon source could be added to the media after inoculation to select only plastic-degrading bacteria.

LDPE, LLDPE, and EPS were cut and subjected to sterilization to ensure no contamination with carbon sources other than plastics according to the method described before. The weight of the plastics was measured before putting them into the designated sample. For positive control (PCB), MS medium supplemented with 0.1% glucose was used. For negative control (NCB), an MS medium with no carbon source was added. Inoculation for the PCB and NCB was done by mixing all the diluted samples (3.3*3 ml) in 250 ml MS medium. The incubation

was done in a shaker incubator at 130 rpm at 37°C. The incubation period was 60 days, and bacterial growth was observed every 7 days.

After 60 days of incubation, 100 µL of the incubated sample was cultured on Nutrient Agar (NA), MacConkey agar, Cetrimide agar, and Mannitol Salt Agar (MSA) using the spread plate method. NA can support a wide range of non-fastidious bacteria and is used as an indicator for the presence of bacteria in the incubated MS broth. The other three media were used due to the focus on *Pseudomonas* - MacConkey agar and Cetrimide agar can selectively grow *Pseudomonas*, whereas MSA does not support its growth (Brown & Lowbury, 1965). The other purpose of MSA was to evaluate if any gram-positive bacteria were growing in MS broth. The bacterial colonies that grew were first isolated and differentiated via colony morphology and selective growth. Then, depending on the different morphology observed among the three designated plastic types, polymerase chain reaction (PCR) was done to confirm the *Pseudomonas* genus with PA-GS primer pairs. For the PCR process, conditions were as described by (Spilker et al., 2004).

In the PCR process, the primer pair used was PA-GS-F and PA-GS-R (Table 1). A total volume of 15 µl (12 µl PCR mix and 3 µl template DNA) was produced. For every sample, the PCR mix included forward primer 1.5 µl, reverse primer 1.5 µl, PCR master mix 7.5 µl and nuclease-free water 1.5 µl. The PCR conditions were as follows, initial denaturation at 95°C for 2 minutes, denaturation at 94°C for 20 seconds, annealing at 54°C for 20 seconds, extension at 72° for 40 seconds, and final extension at 72° for 1 minute. The PCR was run for 30 cycles.

***Table 1**:* 16s rDNA-based primers and their characteristics. Reference: Spilker et al., 2004

Primer	**Sequence (5′-3′)**	**Target**	**Annealing temp (°C)**	**Location**	**Product size (bp)**
PA-GS-F	GACGGGTGAGTAATGCCTA	*Pseudomonas* species	54	95-113	618
PA-GS-R	CACTGGTGTTCCTTCCTATA			693-712	
PA-SS-F	GGGGGATCTTCGGACCTCA	*P. aeruginosa*	58	189-206	956
PA-SS-R	TCCTTAGAGTGCCCACCCG			1124-1144	

2.8 FTIR analysis

Fourier Transform Infrared Spectroscopy (FTIR) was done using a spectrophotometer (IRPrestige-21, SHIMADZU, Japan). This was used to analyze how functional groups were changed upon *Z. atratus* larval consumption (Peng et al., 2020). This analysis was done on fresh LDPE, LLDPE, and EPS (control) as well as after these were consumed as feed, and larvae frass from all the systems.

Firstly the samples were mixed with 30 % hydrogen peroxide (H_2O_2) at 60°C and treated for 3 days to dissolve contaminants. Then the H_2O_2 was removed and the samples were washed with distilled water. After that, 5.3 mol/l of aqueous sodium iodide (NaI) was added to the samples, incubated for 7 hours, and then gravity separation was conducted. The samples were air-dried, and the FTIR machine was used to analyze them. The resolution of analysis was 4 cm^{-1}, and accumulation was done 45 times at a wavelength range of 4000 - 600 cm^{-1}.

2.9 SEM Analysis

Scanning Electron Microscopy (SEM) was performed as previously described (Taghavi et al., 2021) using an ultra-high-resolution Schottky Field Emission Scanning Electron Microscope (JSM-7610F, JEOL, Japan). SEM images were taken after LDPE, LLDPE, and EPS samples were incubated in MS broth with isolated bacteria for two months. Untreated LDPE, LLDPE, and EPS samples were used as controls.

After 2 months of incubation with isolated bacteria, plastics were cut by 1 cm x 1 cm. They were placed in a glass vial and air dried at 50°C for 2 days. Then the fully dried samples were mounted on a suitable specimen stub with carbon tape and coated the sample with a thin layer of platinum using a sputter coater. Now the samples were ready to mount in the SEM machine. For LDPE and LLDPE, the SEM image was captured in 1µm length with 3000x magnification. For EPS, it was captured in 10µm length with 1000x magnification. As different plastic type has different structures, different magnifications and lengths have been adjusted accordingly.

2.10 Whole Genome Sequencing, Assembly, and Species Identification

The confirmed samples for *Pseudomonas* were sent to the International Centre for Diarrhoeal Disease Research, Bangladesh (icddr, b) for Whole Genome Sequencing (WGS). The genomic DNA from the *Pseudomonas* samples was extracted using the Wizard® Genomic DNA Purification Kit (Promega, WI, USA) according to the manufacturer's instructions. WGS of the extracted DNA was performed using the NextSeq 550 Sequencer (Illumina, CA, USA). Illumina DNA prep library kit was used to prepare the genomic fragments before carrying out sequencing with a paired-end layout of 150 bp. Generated paired-end reads were trimmed to remove adapters using DRAGEN Bio-IT Platform. The generated trimmed reads were checked for quality using FastQC (LaMar, 2015). After that, SPAdes 3.15.3 under the Galaxy server was used to assemble the reads (Bankevich et al., 2012). Since the sequencing depth was higher

than 50X for both samples, --isolate option was enabled to generate both contigs and scaffolds. For the identification of species and strains, the assembled genomes were uploaded to PubMLST "Identify Species" tool and searched (Jolley et al., 2018). Furthermore, the annotated 16S ribosomal RNA (rRNA) sequences from the genomes were compared with known 16S rRNA sequences using NCBI BLASTN (Altschul et al., 1990). Finally, PA-SS primers were used to carry out species-specific PCR for *P. aeruginosa*, and the amplicons were analyzed in agarose gel electrophoresis (Spilker et al., 2004).

In the PCR process, the primer pair used was PA-SS-F and PA-SS-R (Table 1). A total volume of 15 µl (12 µl PCR mix and 3 µl template DNA) was produced. For every sample, the PCR mix included forward primer 1.5 µl, reverse primer 1.5 µl, PCR master mix 7.5 µl and nuclease-free water 1.5 µl. The PCR conditions were as follows, initial denaturation at 95°C for 2 minutes, denaturation at 94°C for 20 seconds, annealing at 58°C for 20 seconds, extension at 72° for 40 seconds, and final extension at 72° for 1 minute. The PCR was run for 30 cycles.

To determine the MLST (Multilocus Sequence Typing) type, the assembled genomes were uploaded to the PubMLST *P. aeruginosa* typing database for analyzing MLST loci. The typing is based on an allelic profile composed of 7 separate loci: *acsA, aroE, quaA, mutL, nuoD, ppsA*, and *trpE*. The assembly quality of the contigs and scaffolds was analyzed using QUAST 5.2.0 (Gurevich et al., 2013). Reference genome FASTA file and GFF (General Feature Format) file for *P. aeruginosa* were provided for improved assessment. Assembled genomes were analyzed with the MOB-Recon 3.0.3 under the Galaxy server to identify possible plasmid sequences (Robertson & Nash, 2018). Matched plasmid sequences were retrieved and compared with the assembled sequences using BLASTN. The assemblies were submitted to NCBI SRA (Sequence Read Archive).

2.11 Genome Annotation and Analysis

For annotation, the assembled genomes were annotated using Prokka 1.14.6 under the Galaxy Europe server, with species specified as *P. aeruginosa* and genus-specific BLAST database enabled (Seemann, 2014). To check for genome completeness, the assembled genomes were compared against a set of 1617 marker genes using the CheckM taxonomy workflow under the Galaxy Europe server (Parks et al., 2015). The assembled genome and the associated GFF3 files were provided to Operon-mapper to predict potential operons throughout the genomes (Taboada et al., 2018). Proteins were also uploaded to the BLASTKoala server to assign K numbers to the proteins (Kanehisa et al., 2016).

Moreover, to identify potential plastic-degrading enzymes among the annotated proteins, the protein sequences predicted from each genome were uploaded to the PlasticDB "Annotate genome" tool for BLASTP analysis against sequences of known plastic-degrading enzymes (Gambarini et al., 2022). Additionally, to find possible antibiotic resistance genes in the genomes, the assembled genomes were uploaded to CARD-RGI (Comprehensive Antibiotic Resistance Database - Resistance Gene Identifier) to find matches with known antibiotic resistance genes (Alcock et al., 2023). The comparison looked for perfect matches as well as strict matches with over 95% identity. Lastly, to identify possible virulence factors, the protein sequences predicted from each genome were uploaded to VFanalyzer; the genus was specified as *Pseudomonas* (Chen et al., 2005).

For pan-genome analysis, the RefSeq genome assemblies of the following *P. aeruginosa* strains were retrieved from NCBI: biosurfactant producing strains UCBPP-PA14 and PA7; PE degrading strain E7; LDPE degrading strain PA01; highly virulent strains PA14_ASM2549037, PA14_ASM2549039, PA14_ASM2549041, and PA14_ASM2549047; and BWHPSA013, which has the same MLST type as the assembled genomes (Gutiérrez-Gómez et al., 2019; Jeon & Kim, 2015; Kyaw et al., 2012; Lee et al., 2006; Toribio et al.,

2010). The genomes were annotated with Prokka as before and then compared with the annotated genomes using Roary 3.13.0 under Galaxy Europe server, with BLASTP cutoff set at 99% (Page et al., 2015). For further confirmation, proteins of interest were further analyzed at InterProScan for identification of motifs and domains (Paysan-Lafosse et al., 2023).

16S rRNA sequences that showed more than 97% sequence identity with sequences from both isolates were retrieved from NCBI. The 16S rRNA sequences from the Prokka-annotated *P. aeruginosa* strains were also retrieved. All 16S rRNA sequences were submitted to the NGPhylogeny web service for phylogenetic tree construction (Lemoine et al., 2019). The sequences were aligned using MAFFT, followed by alignment curation using BMGE, tree inference using PhyML+SMS, and finally, tree rendering using Newick display (Criscuolo & Gribaldo, 2010; Guindon et al., 2010; Junier & Zdobnov, 2010; Katoh & Standley, 2013; Lefort et al., 2017; Lemoine et al., 2018). The rendered tree was visualized and modified in Interactive Tree Of Life (iTOL) (Letunic & Bork, 2021). Additionally, a core gene alignment was generated by Roary, which was analyzed through a similar pipeline to render and visualize a phylogenetic tree of the strains.

2.12 Bio-surfactant Assay

Biosurfactant assay were done to see whether the isolated bacteria could produce any biosurfactant that can be used during oil spill bioremediation. In this assay, paraffin oil was used. This assay had two tests: the oil spread test and the drop collapse test. For these tests, 48 H cultures were produced. In addition to these cultures, a 4-month-old bacteria culture (using nutrient broth with LDPE, LLDPE, and EPS) and 1 Year 1-year-old bacteria culture (using MSB media with plastics as sole carbon source) were tested.

Now 9 systems were designed,

i. Nutrient broth inoculated with bacteria

ii. Nutrient broth inoculated with bacteria and added soybean oil

iii. Nutrient broth inoculated with bacteria added paraffin oil

iv. Nutrient broth (Negative control)

v. Nutrient broth (Negative control)

vi. 4 month old bacteria culture+ Nutrient broth+ soybean oil

vii. 4 month old bacteria culture+ Nutrient broth+ paraffin oil

viii. 4-month-old bacteria culture

ix. 1-Year-old bacteria culture

Here, soybean oil and paraffin oil in the culture tubes increase stress on the inoculated bacteria. It is hoped that they will produce more biosurfactants due to the environmental stress.

2.12.1 Oil Spread Test

An oil spread test was done with all the systems. First, 1 ml of cultures from all the systems were collected and centrifuged at 5000 rpm for 10 minutes. Culture supernatant was collected. Next, in a petri dish, 20ml water was poured. In the water, 2 ml of paraffin oil was added. Now, 1ml culture supernatant was added on top of the oil at the center of the petri dish. If the oil produced zone, it meant the culture supernatant contained biosurfactant whereas no zone means no biosurfactant. As a positive control, 10% Triton X-100 was used.

2.12.2 Drop Collapse Test

A drop collapse test was done with all the systems. In a vial, 1 ml of paraffin oil was taken. Then, 500µl culture was added. The result was observed after 1 minute. If the culture drop was flat or seemed like it was mixing with oil, then it was a positive result. If the culture drop was round with a clear shape, then it was a negative result. Here, as a positive control, 10% Triton X-100 was used.

2.13 Antimicrobial Susceptibility Test

Antimicrobial susceptibility tests were performed from the WGS data. According to the WGS data for AMR genes, antibiotics from different classes were chosen. Firstly, isolated bacteria were grown on nutrient agar media. Mueller–Hinton agar was used for AST. With 24H culture, 0.5 McFarland standard solutions were prepared. Using a sterile cotton swab, bacteria were inoculated with the lawn method. AST was done using the disk diffusion procedure. So, the disks of the selected antibiotics were put on the surface of the media. The culture incubation period was 24 hours at 37° C. After incubation, the zone was measured (diameter in mm) according to CLSI guidelines.

2.14 Statistical Analysis

The analysis of plastic consumption and survivability were assessed by one-way ANOVA coupled with Tukey's honest significant difference (HSD) post-hoc test. The analysis was performed via GraphPad Prism version 8 (GraphPad Software, MA, USA).

Chapter 3

Results

3.1 *Zophobas atratus* Plastic Consumption Rate and Survival Rate

The larvae excreted brown particle-like frass. The frass contained a trace amount of plastics, however as the larvae can recycle the frass, as time passed, the amount of plastic particles also decreased. On another note, larvae showed cannibalism. Though in most of the system, dead larvae were removed as soon as possible, some started cannibalization. On the other hand, molting was seen in all systems (Figure 1). Among all the systems, only two larvae became pupae, and they successfully became adult insects after isolating them from the rest of the group (Figure 1). Of the two adults, one was male and one was female (Figure 1).

The larvae consumed all three types of plastics (Figure 4). However, the degree of consumption is different. PC for LLDPE was on average 15.12% in 36 days, with 0.41 mg 20 larvae^{-1} day^{-1} (Figure 5). The SR for this group was found to be 87% ± 10.4% (Figure 6). Similarly, the PC for the larvae feeding on LDPE was on average 24.04% in 36 days with 7.37 mg 20 larvae^{-1} day^{-1} with 85% ± 10% SR (Figure 5, 6). For EPS, the PC was on average 20.01% in 36 days with 12.39 mg 20 larvae^{-1} day^{-1} (Figure 5). The SR for this group was found to be 90% ± 8.66% (Figure 6). In PCN, the SR was 100%, whereas NCN had 68% ± 7.63% (Figure 6). For all the groups except the PCN, the LW decreased over time (Figure 3). When compared with PCN LW, significant change can be observed from 36 days onwards for LDPE and EPS and from 24 days onwards for LLDPE (Table 2). However, there is no significant difference in LW decrease among the three plastic types.

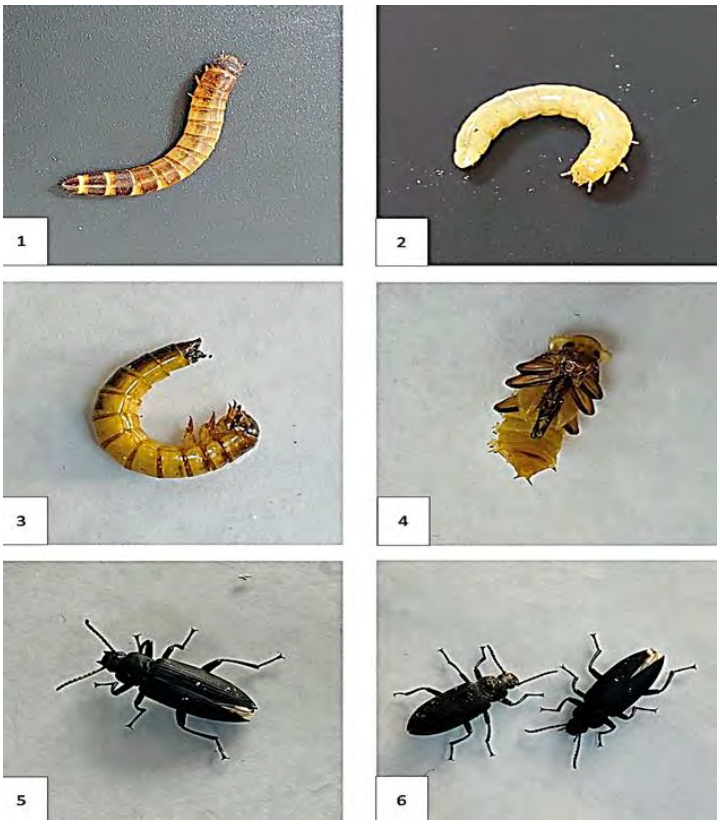

Figure 1: The larvae lifecycle observed during experimentation. (1) Larvae. (2) Larvae after molting. (3) Pre-pupae stage. (4) Pupae stage. (5) Adult beetle. (6) Male and female beetle

Figure 2: Larvae frass. The larvae excreted brown particle like frass

Table 2: Larvae Weight measurement for 51 days (average of triplicated results).

Days	PCN LW (g)	NCN LW (g)	LLDPE LW (g)	LDPE LW (g)	EPS LW (g)
0	0.392±0.017	0.387±0.023	0.367±0.013	0.392±0.017	0.413±0.0066
21	0.434±0.054	0.35±0.028	0.345±0.039	0.362±0.040	0.355±0.0385
24	0.443±0.057	0.339±0.025	0.344±0.049*	0.354±0.036	0.357±0.036
36	0.466±0.061	0.318±0.016	0.335±0.029*	0.329±0.048*	0.339±0.0370*
41	0.480±0.055	0.304±0.017	0.332±0.057*	0.317±0.054*	0.326±0.045*
51	0.516±0.043	0.273±0.016	0.331±0.058*	0.303±0.069*	0.319±0.043*

*= significant value ($p<0.05$) when compared with PCN LW. No significant LW change when compared with NCN LW. SR of NCN was the lowest among the tests, which implies plastic consumption gave enough nutrients to the larvae to survive more. PCN=positive control, NCN=negative control, LW= larvae average weight, LLDPE= linear low density polyethylene, LDPE=low density polyethylene, EPS=expanded polystyrene

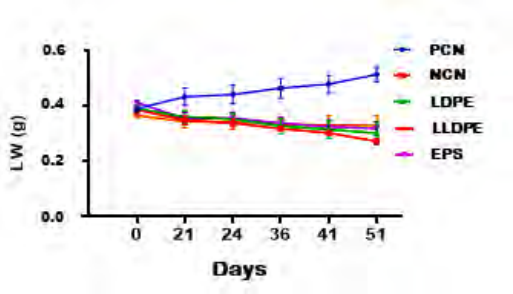

Figure 3: Time analysis of LW. When compared with PCN LW, significant ($p < 0.05$) change can be observed from 36 days onwards for LDPE and EPS and from 24 days onwards for LLDPE. No significant difference in LW decrease among LDPE, EPS, and LLDPE

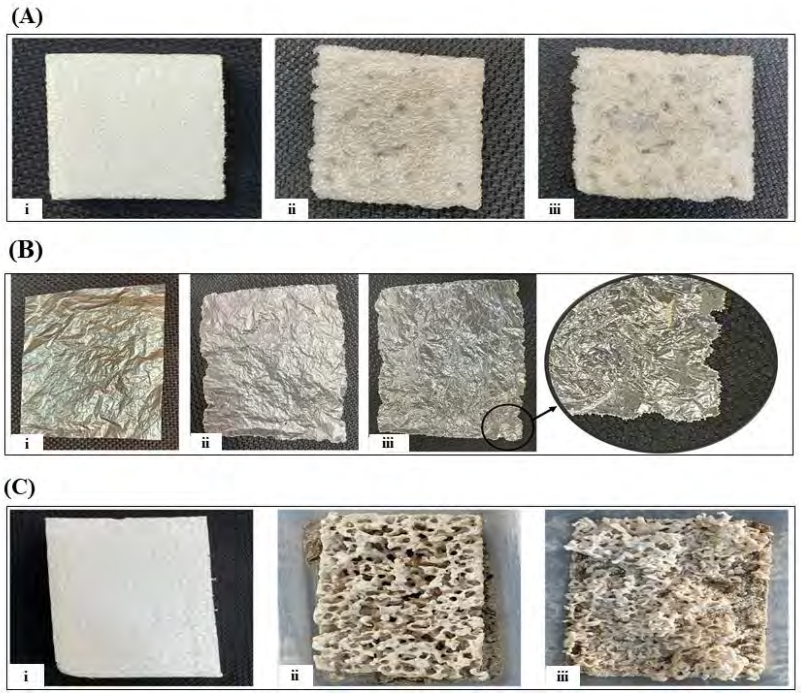

Figure 4: Larvae consumed all 3 types of plastic. (A) LDPE consumption by the larvae in 36 days, (i) control LDPE, (ii) after 15 days, (iii) after 36 days. (B) LLDPE consumption by the larvae in 36 days, (i) control LLDPE, (ii) after 36 days, (iii) close-up shot in for a better view. (C) EPS consumption by the larvae in 51 days, (i) control EPS, (ii) after 36 days, (iii) after 51 days. LLDPE=linear low-density polyethylene, LDPE=low density polyethylene, EPS=expanded polystyrene

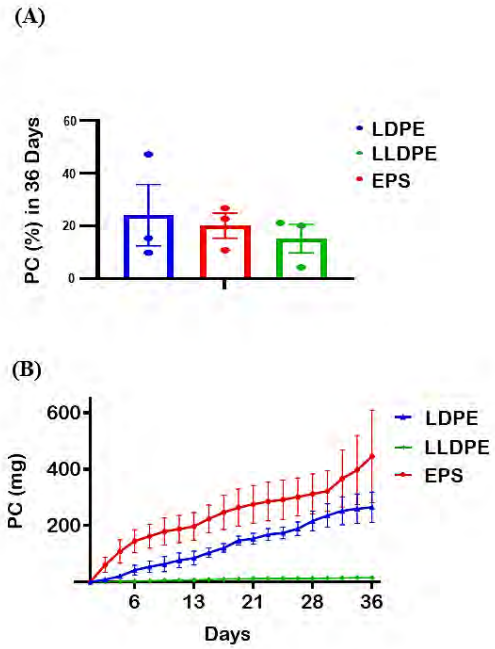

Figure 5: The larvae consumed the plastics at various rates. (A) PC with different plastic types (triplicated result) where LDPE has the highest rate and LLDPE has the lowest. (B) PC with a time analysis of 36 days. The points represent the mean ± SEM (n = 3). Data were analyzed using one-way ANOVA coupled with Tukey's honest significant difference (HSD) posthoc test

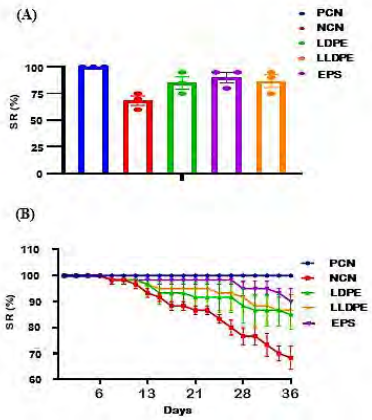

Figure 6: Larvae survivability showed EPS as the best plastic type. (A) SR%. PCN had 100 % SR and NCN had 68 %. Among the plastic types, EPS had the highest SR whereas LDPE had the lowest. (B) Time analysis of SR% in 36 days. In all the statistical analyses, the points represent the mean ± SEM (n = 3). Data were analyzed using one-way ANOVA coupled with Tukey's honest significant difference (HSD) post-hoc test. SR = survival rate, PCN = positive control, NCN = negative control, LW = larvae average weight, LLDPE = linear low-density polyethylene, LDPE = low density polyethylene, EPS = expanded polystyrene

3.2 FTIR Analysis

FTIR analysis showed proof of oxidation in the gut. As stated earlier, fresh plastic (as a control), larvae consumed plastic, and larvae frass were analyzed for each system. New functional groups at 1075-1150 cm^{-1} (-C-O stretch), 1700 cm^{-1} (-C=O stretch), and 3440 cm^{-1} (Re-OH stretch) wavenumbers were identified (Figure 7). For all three plastic types, these three functional groups were only found in the frass whereas control and consumed plastics had almost similar results. In the control and consumed plastics, no oxygen bonded with another element was identified. Additionally for LDPE, 1700 cm^{-1} (-C=O stretch) peak was also found in the consumed part which was absent in the control.

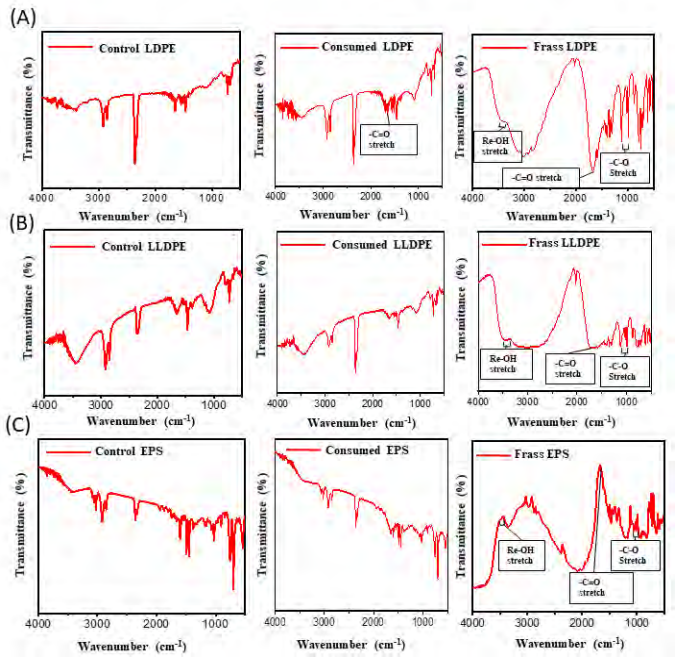

Figure 7: FTIR analysis where three new 1075-1150 cm^{-1} (-C-O stretch), 1700 cm^{-1} (-C=O stretch), and 3440 cm^{-1} (Re-OH stretch) functional groups were found which proves oxidation. (A) Analysis of LDPE. Consumed LDPE had –C=O stretch and frass had all three but control had none of the functional groups of those three. (B) Analysis of LLDPE. Control and consumed had similar results whereas frass had three new functional groups. (C) Analysis of EPS, control, and consumed had none of those three functional groups but frass had. LLDPE=linear low-density polyethylene, LDPE=low density polyethylene, EPS=expanded polystyrene

3.3 Bacteria Isolation and Identification

Growth was observed after inoculation in MSB from every system every 7 days. After 7 days, no growth was observed for NCB. For PCB, no growth was observed after 40 days. After 60 days of incubation, spread plating was done on selective media, where NA, MacConkey agar, and Cetrimide agar showed bacterial growth. As the target bacteria was *Pseudomonas*, growth on cetrimide agar plate was chosen. Isolated bacteria from LDPE/LLDPE gave a green pigmentation without UV whereas bacteria from EPS gave no color (Figure 8). However, both isolates exhibited florescence under UV. Due to similar types of plastic and morphology, isolates grown on LDPE/LLDPE were designated as "PDB-1" and the isolate grown on EPS was designated as "PDB-2". These two isolates were confirmed *Pseudomonas* with PCR which gave its characteristic band in gel electrophoresis.

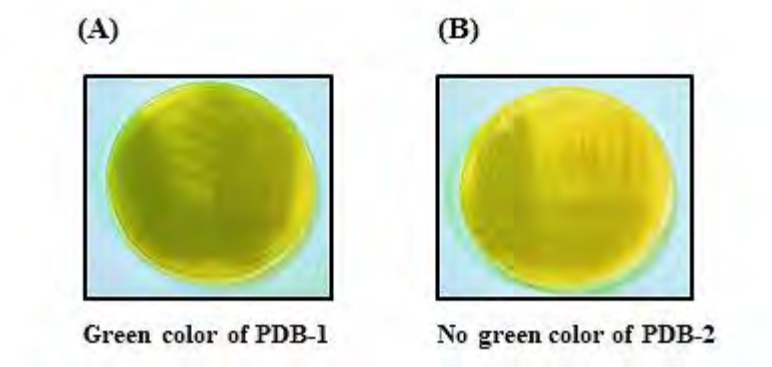

Figure 8: Isolated bacteria characteristics. Bacteria from LDPE and LLDPE media displayed green pigmentation without UV, while those from EPS media lacked this pigmentation. All exhibited fluorescence under UV, a positive *Pseudomonas* characteristic. Isolates PDB-1 (from LDPE and LLDPE) and PDB-2 (from EPS) demonstrated growth in MS medium with specific plastics as the sole carbon source, indicating plastic-degrading biochemical pathways. In the figure (A) green pigmentation for PDB-1, (B) no green pigmentation for PDB-2.

3.4 SEM Analysis

Both PDB-1 and PDB-2 had shown surface degradation as seen using SEM. In this analysis, LDPE and LLDPE were incubated with PDB-1 and EPS with PDB-2 in MSB broth where the plastics were the sole carbon source. After incubation, all incubated plastics showed signs of surface degradation when compared with controls. The control samples exhibited smooth surfaces, while the incubated samples displayed rough, fragmented surfaces characterized by the presence of bacteria and biofilms. In the case of LDPE, control samples showed minor irregularities with isolated microplastic particles, whereas the incubated LDPE exhibited surface erosion, featuring significant pits, bumps, microplastic fragments, and biofilm formation. Though images were taken in different lengths with different magnifications, for consistency and to understand better, the image that was captured in 1µm length with 3,000x magnification has been added here (Figure 9). Similarly, LLDPE control samples demonstrated smooth surfaces, contrasting with the rough, bumpy surfaces of the incubated samples, accompanied by bacterial colonization and biofilm formation. Though images were taken in different lengths with different magnifications, for consistency and to understand better, the image that was captured in 1µm length with 10,000x magnification has been added here (Figure 9). Likewise, EPS control samples displayed smooth surfaces, whereas the incubated EPS exhibited tears, holes, and biofilm formation at various locations. Though images were taken in different lengths with different magnifications, for consistency and to understand better, the image that was captured in 10µm length with 1,000x magnification has been added here (Figure 9).

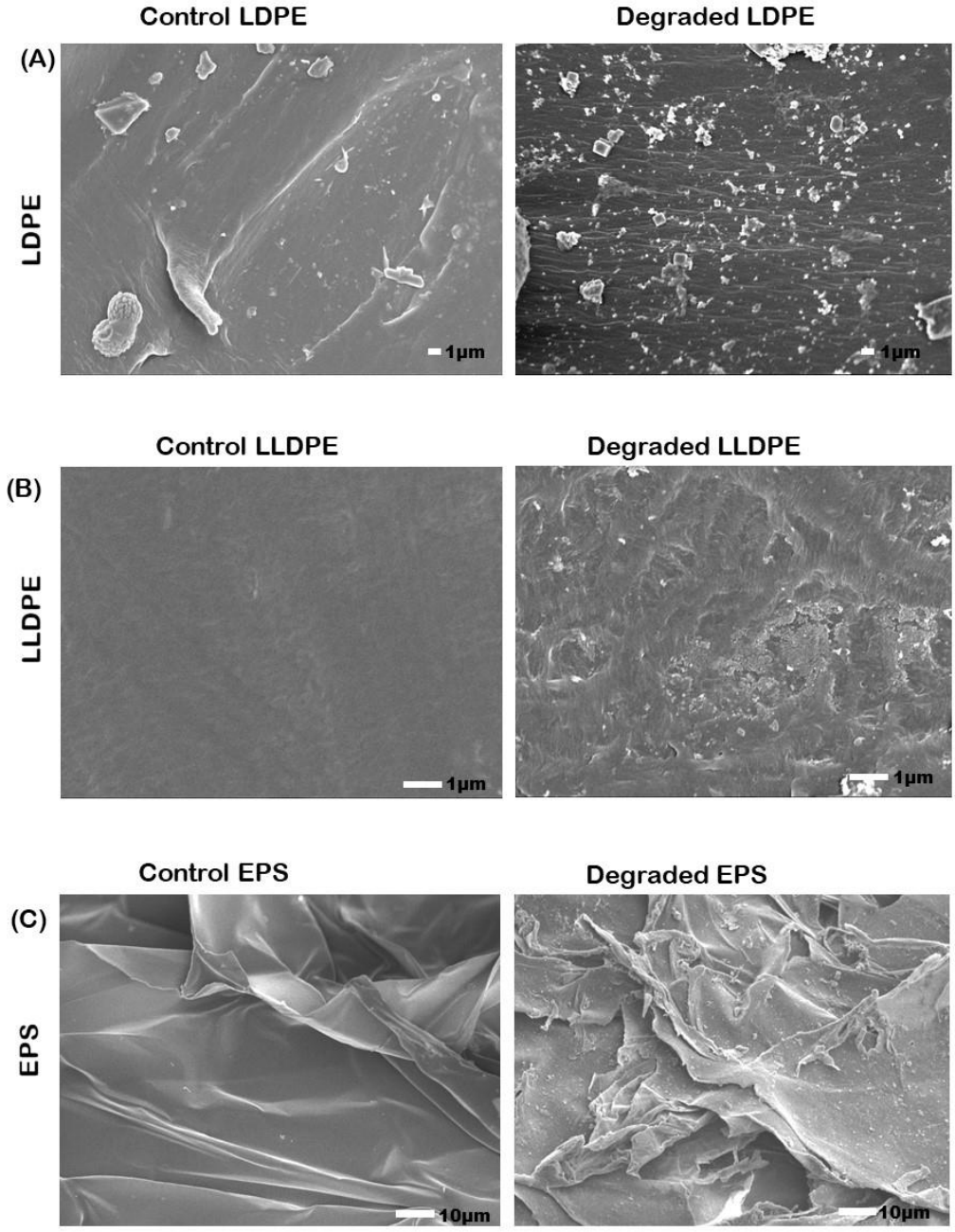

Figure 9: SEM analysis of LDPE, LLDPE and EPS proved degradation by the two isolated bacteria. (A) Control and degraded LDPE by PDB-1 isolate. Control had a comparatively smooth surface with little microplastics whereas degraded LDPE had a rough surface with many microplastics. The image was captured in 1µm length with 3000x magnification. (B) Control and degraded LLDPE by PDB-1 isolate. Control had a smooth surface whereas degraded LLDPE had a rough surface with bacteria and biofilms. The image was captured in 1µm length with 10000x magnification. (C) Control and degraded EPS by PDB-2 isolate. Control had a smooth surface whereas degraded EPS had a rough surface with tears, holes, and biofilms. The image was captured in 10µm length with 1000x magnification. LLDPE= linear low-density polyethylene, LDPE=low density polyethylene, EPS=expanded polystyrene

3.5 Genome Assembly and Identification

According to the sequencing data, PDB-1 and PDB-2 were sequenced with coverages of 298.7 and 142.1, respectively. Upon assembly, PDB-1 yielded 2254 contigs and 2164 scaffold assemblies, with 152 contigs and 62 scaffolds exceeding 500 bp in length. Conversely, the PDB-2 assembly generated 1218 contigs and 1133 scaffold assemblies, with 140 contigs and 55 scaffolds over 500 bp in length. The NG50 value for PDB-1 contigs was 81867 bps, increasing to 246604 bps for the scaffolds. Similarly, PDB-2 contigs had an NG50 value of 87657 bps, rising to 258807 bps for the scaffolds. Scaffolds exhibited slightly higher genome coverage than contigs in both cases, thus chosen as the genomic sequence. The assemblies' quality was indicated by the low contig count (<100) and high NG50 value (>50000bp). The assemblies are available in NCBI under **BioProject ID PRJNA1005894**.

PubMLST identified the genome as *P. aeruginosa* with 100% confidence, showing 55 exact matches with known sequences. NCBI BLASTN revealed nearly identical 16S rRNA sequences to known *P. aeruginosa* sequences, and as both isolates have identical 16s rRNA sequences, it suggests a close phylogenetic relationship. Additionally, PCR with PA-SS primer pairs confirmed their identity as *P. aeruginosa* (Figure 10). Furthermore, MLST typing classified the genomes as ST170 (Loci numbers - acsA:36, aroE:5, quaA:29, mutL:7, nuoD:4, ppsA:10, and trpE:7).

Lastly, MOB-Recon analysis detected probable plasmid sequences in both genomes, matching with known *P. aeruginosa* plasmid sequences. Plasmid pHOU1-1 from *P. aeruginosa* strain HOU1 matched scaffold sequences from both genomes. Comparison with the plasmid sequence (GenBank Accession: CP042268) identified 2 scaffold sequences from PDB-1 and 3 scaffold sequences from PDB-2 as probable plasmid sequences.

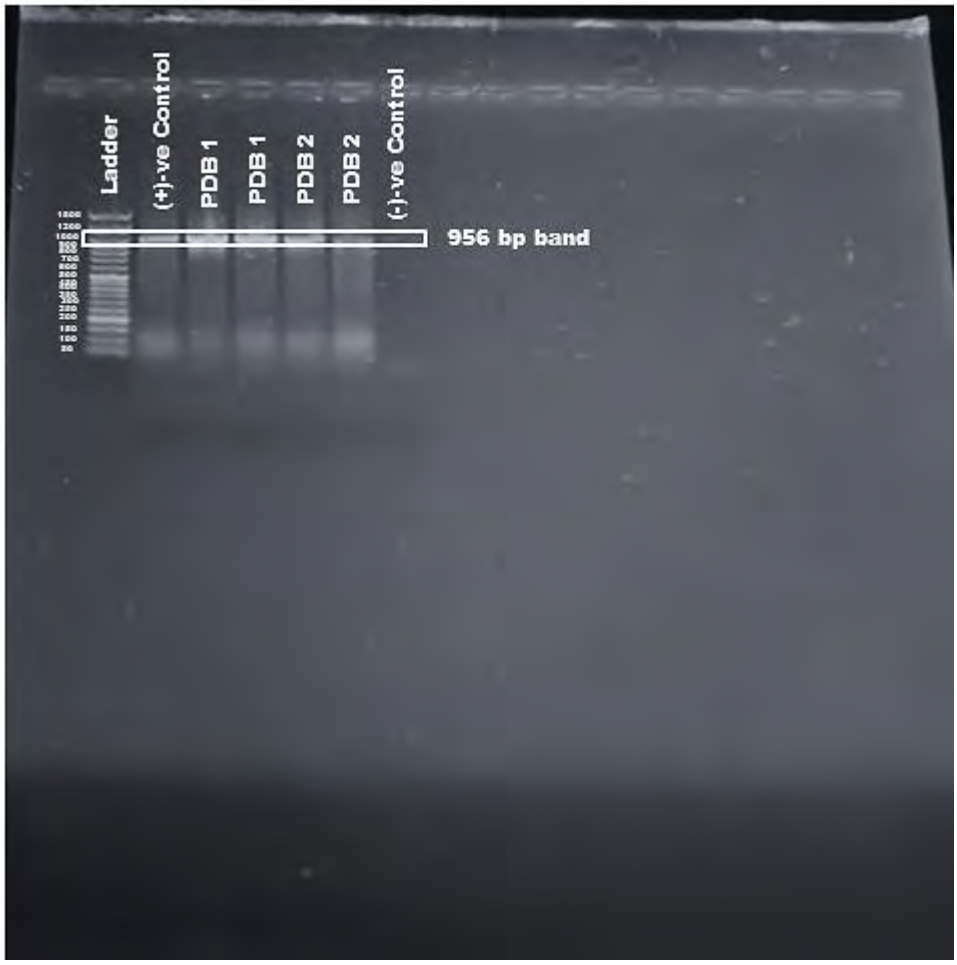

Figure 10: Isolated bacteria characteristics. Gel electrophoresis using PA-SS primer set with characteristic DNA band at 956 bp. (+)-ve control had already identified *P. aeruginosa* whereas (-)-ve control had no sample DNA. All the bands for PDB-1 and PDB-2 aligned at 956 bp along with the (+)-ve control which is the characteristic of *P. aeruginosa* . No band at (-)-ve control means there was no contamination during the experimentation. The DNA ladder used during gel electrophoresis was AMPIGENE® DNA Ladder 50-1,500 bp.

PDB-1 and PDB-2 16s rDNA sequences are given below:

>PDB1_16S ribosomal RNA

TGAAGAGTTTGATCATGGCTCAGATTGAACGCTGGCGGCAGGCCTAACACATGCAAGTCG

AGCGGATGAAGGGAGCTTGCTCCTGGATTCAGCGGCGGACGGGTGAGTAATGCCTAGGAA

TCTGCCTGGTAGTGGGGGATAACGTCCGGAAACGGGCGCTAATACCGCATACGTCCTGAG

GGAGAAAGTGGGGGATCTTCGGACCTCACGCTATCAGATGAGCCTAGGTCGGATTAGCTA

GTTGGTGGGGTAAAGGCCTACCAAGGCGACGATCCGTAACTGGTCTGAGAGGATGATCAG

TCACACTGGAACTGAGACACGGTCCAGACTCCTACGGGAGGCAGCAGTGGGGAATATTGG

ACAATGGGCGAAAGCCTGATCCAGCCATGCCGCGTGTGTGAAGAAGGTCTTCGGATTGTA

AAGCACTTTAAGTTGGGAGGAAGGGCAGTAAGTTAATACCTTGCTGTTTTGACGTTACCA

ACAGAATAAGCACCGGCTAACTTCGTGCCAGCAGCCGCGGTAATACGAAGGGTGCAAGCG

TTAATCGGAATTACTGGGCGTAAAGCGCGCGTAGGTGGTTCAGCAAGTTGGATGTGAAAT

CCCCGGGCTCAACCTGGGAACTGCATCCAAAACTACTGAGCTAGAGTACGGTAGAGGGTG

GTGGAATTTCCTGTGTAGCGGTGAAATGCGTAGATATAGGAAGGAACACCAGTGGCGAAG

GCGACCACCTGGACTGATACTGACACTGAGGTGCGAAAGCGTGGGGAGCAAACAGGATTA

GATACCCTGGTAGTCCACGCCGTAAACGATGTCGACTAGCCGTTGGGATCCTTGAGATCT

TAGTGGCGCAGCTAACGCGATAAGTCGACCGCCTGGGGAGTACGGCCGCAAGGTTAAAAC

TCAAATGAATTGACGGGGGCCCGCACAAGCGGTGGAGCATGTGGTTTAATTCGAAGCAAC

GCGAAGAACCTTACCTGGCCTTGACATGCTGAGAACTTTCCAGAGATGGATTGGTGCCTT

CGGGAACTCAGACACAGGTGCTGCATGGCTGTCGTCAGCTCGTGTCGTGAGATGTTGGGT

TAAGTCCCGTAACGAGCGCAACCCTTGTCCTTAGTTACCAGCACCTCGGGTGGGCACTCT

AAGGAGACTGCCGGTGACAAACCGGAGGAAGGTGGGGATGACGTCAAGTCATCATGGCCC

TTACGGCCAGGGCTACACACGTGCTACAATGGTCGGTACAAAGGGTTGCCAAGCCGCGAG

GTGGAGCTAATCCCATAAAACCGATCGTAGTCCGGATCGCAGTCTGCAACTCGACTGCGT

GAAGTCGGAATCGCTAGTAATCGTGAATCAGAATGTCACGGTGAATACGTTCCCGGGCCT

TGTACACACCGCCCGTCACACCATGGGAGTGGGTTGCTCCAGAAGTAGCTAGTCTAACCG

CAAGGGGGACGGTTACCACGGAGTGATTCATGACTGGGGTGAAGTCGTAACAAGGTAGCC

GTAGGGGAACCTGCGGCTGGATCACCTCCTT

>PDB2_16S ribosomal RNA

TGAAGAGTTTGATCATGGCTCAGATTGAACGCTGGCGGCAGGCCTAACACATGCAAGTCG

AGCGGATGAAGGGAGCTTGCTCCTGGATTCAGCGGCGGACGGGTGAGTAATGCCTAGGAA

TCTGCCTGGTAGTGGGGGATAACGTCCGGAAACGGGCGCTAATACCGCATACGTCCTGAG

GGAGAAAGTGGGGGATCTTCGGACCTCACGCTATCAGATGAGCCTAGGTCGGATTAGCTA

GTTGGTGGGGTAAAGGCCTACCAAGGCGACGATCCGTAACTGGTCTGAGAGGATGATCAG

TCACACTGGAACTGAGACACGGTCCAGACTCCTACGGGAGGCAGCAGTGGGGAATATTGG

ACAATGGGCGAAAGCCTGATCCAGCCATGCCGCGTGTGTGAAGAAGGTCTTCGGATTGTA

AAGCACTTTAAGTTGGGAGGAAGGGCAGTAAGTTAATACCTTGCTGTTTTGACGTTACCA

ACAGAATAAGCACCGGCTAACTTCGTGCCAGCAGCCGCGGTAATACGAAGGGTGCAAGCG

TTAATCGGAATTACTGGGCGTAAAGCGCGCGTAGGTGGTTCAGCAAGTTGGATGTGAAAT

CCCCGGGCTCAACCTGGGAACTGCATCCAAAACTACTGAGCTAGAGTACGGTAGAGGGTG

GTGGAATTTCCTGTGTAGCGGTGAAATGCGTAGATATAGGAAGGAACACCAGTGGCGAAG

GCGACCACCTGGACTGATACTGACACTGAGGTGCGAAAGCGTGGGGAGCAAACAGGATTA

GATACCCTGGTAGTCCACGCCGTAAACGATGTCGACTAGCCGTTGGGATCCTTGAGATCT

TAGTGGCGCAGCTAACGCGATAAGTCGACCGCCTGGGGAGTACGGCCGCAAGGTTAAAAC

TCAAATGAATTGACGGGGGCCCGCACAAGCGGTGGAGCATGTGGTTTAATTCGAAGCAAC

GCGAAGAACCTTACCTGGCCTTGACATGCTGAGAACTTTCCAGAGATGGATTGGTGCCTT

CGGGAACTCAGACACAGGTGCTGCATGGCTGTCGTCAGCTCGTGTCGTGAGATGTTGGGT

TAAGTCCCGTAACGAGCGCAACCCTTGTCCTTAGTTACCAGCACCTCGGGTGGGCACTCT

AAGGAGACTGCCGGTGACAAACCGGAGGAAGGTGGGGATGACGTCAAGTCATCATGGCCC

TTACGGCCAGGGCTACACACGTGCTACAATGGTCGGTACAAAGGGTTGCCAAGCCGCGAG

GTGGAGCTAATCCCATAAAACCGATCGTAGTCCGGATCGCAGTCTGCAACTCGACTGCGT

GAAGTCGGAATCGCTAGTAATCGTGAATCAGAATGTCACGGTGAATACGTTCCCGGGCCT

TGTACACACCGCCCGTCACACCATGGGAGTGGGTTGCTCCAGAAGTAGCTAGTCTAACCG

CAAGGGGGACGGTTACCACGGAGTGATTCATGACTGGGGTGAAGTCGTAACAAGGTAGCC

GTAGGGGAACCTGCGGCTGGATCACCTCCTT

3.6 Annotation of Significant Genes

During the annotation process, PDB-1 and PDB-2 revealed 6011 and 5949 putative genes, respectively, with 5859 and 5804 identified as protein-coding sequences. Moreover, out of the 1617 marker genes in CheckM, 1610 and 1611 were detected in PDB-1 and PDB-2, respectively, indicating completeness levels of 99.64% and 99.66%, respectively. Annotations were provided alongside the assembly at NCBI. BLASTKoala analysis assigned K numbers to 3365 and 3359 proteins from PDB-1 and PDB-2, respectively. When predicted proteins were compared with known plastic-degrading proteins in PlasticDB, four predicted proteins from PDB-1 matched PE-degrading enzymes. Specifically, PDB1_00173 and PDB1_01428 matched with *Psychrobacter* sp. laccase (PlasticDB Protein ID: 00180), while PDB1_00445 and PDB1_02915 matched with *Pseudomonas* sp. alkane hydroxylase (PlasticDB Protein ID: 00061), with the latter two also matching LDPE-degrading enzyme alkane monooxygenase from *Paenibacillus* sp. (PlasticDB Protein ID: 00104). No proteins from PDB-2 matched with known PS-degrading enzymes. In a comparison of genes across strains, 1822 core genes were identified as conserved in all strains, alongside 3232 soft core genes, 1758 shell genes, and 5563 cloud genes, which show varying degrees of conservation across different strains.

Phylogenetic analysis based on 16S rRNA sequences indicated that both PDB-1 and PDB-2 isolates formed close clusters with other strains of *P. aeruginosa*. Additionally, strains of various other *Pseudomonas* species and some species from the recently suggested *Stutzerimonas* genus exhibited high sequence similarity. A more robust phylogenetic tree was constructed using core gene alignment from pan-genome analysis, revealing that PDB-1 and PDB-2 shared the highest similarity with the BWHPSA013 strain, which belongs to the same MLST type (Figure 11).

Among the genes in PDB-1, PDB1_05091 was annotated as the Cytochrome P450 107B1 gene, with P450-driven monooxygenase activity essential for the degradation pathway. Additionally,

genes PDB1_01395, PDB1_01396, and PDB1_01397, annotated as short-chain dehydrogenase, esterase, and Baeyer-Villiger monooxygenase, respectively, were predicted to belong to the same operon. Another operon included PDB1_00458 and PDB_00459, annotated as short-chain alcohol dehydrogenase and Baeyer-Villiger monooxygenase, respectively. Furthermore, PDB1_01294, PDB1_01369, and PDB1_03409 were annotated as alcohol dehydrogenases.

PDB1_00173 was annotated as a laccase, supported by PlasticDB. Genes PDB1_00445 and PDB1_02915 were predicted to encode this enzyme, corroborated by PlasticDB. Comparison with genes from the PE-degrading strain E7, LDPE-degrading strain PA01, and PDB-2 revealed orthologs in most cases with over 99% sequence similarity. However, PDB1_01395 and PDB1_01294 did not have orthologs in E7. PDB1_01395 matched only with orthologs from PDB-2, PA01, and BWHPSA013, while PDB1_01294 matched only with orthologs from PDB-2 and PA01. The annotation of the PA7 strain identified a dye-decolorizing peroxidase (yfeX), corresponding to the protein PSPA7_2468 (GenBank Accession: ABR83505), previously annotated as a hypothetical protein.

The gene PDB2_04415 in PDB-2 is annotated as phenylacetaldehyde dehydrogenase (styD), with highly similar orthologs in all other strains except PA7. Conversely, PDB2_05770, also annotated as phenylacetaldehyde dehydrogenase, lacks such orthologs, but the encoded protein is too short to be independently functional. Both PDB2_04415 and PDB2_05770 proteins match with Streptomyces sp. PEG aldehyde dehydrogenase from PlasticDB (PlasticDB Protein ID: 00035). Among PDB-2 genes, PDB2_03471 is annotated as the Cytochrome P450 107B1 gene, orthologous to PDB1_05091. Additionally, both PDB2_03017 and PDB2_03887 genes are annotated as alkane hydroxylases, with their proteins matching with *Pseudomonas* sp. alkane hydroxylase and *Paenibacillus* sp. alkane monooxygenase in PlasticDB.

In PDB-1, RGI identified 25 perfect matches with antibiotic resistance genes, while in PDB-2, 24 perfect matches were found. Most resistance was against fluoroquinolone-, tetracycline-, and phenicol-class antibiotics, with antibiotic efflux being the most common resistance mechanism (Table 3).

Virulence factors present in the isolates were analyzed and compared with other strains. Different genes for adherence, flagella, antiphagocytic activity, etc have been found in both isolates and an important pathway involved in the production of rhamnolipid, a biosurfactant, was identified with three genes, rhlA, rhlB, and rhlC (Table 4).

Table 3: Genes in isolates PDB-1 and PDB-2 showing perfect matches with known Antimicrobial Resistance (AMR) genes, as identified by CARD RGI

Sl	**Isolate**	**Protein_ID**	**Best_Hit_ARO**	**Drug Class**	**Resistance Mechanism**	**AMR Gene Family**
1	PDB-1	PDB1_00081 hypothetical protein	MexL	macrolide antibiotic; tetracycline antibiotic; disinfecting agents and antiseptics	antibiotic efflux	resistance-nodulation-cell division (RND) antibiotic efflux pump
2	PDB-1	PDB1_00229 Sec translocon accessory complex subunit YajC	YajC	fluoroquinolone antibiotic; cephalosporin; glycylcycline; penam; tetracycline antibiotic; oxazolidinone antibiotic; glycopeptide antibiotic; rifamycin antibiotic; phenicol antibiotic;	antibiotic efflux	resistance-nodulation-cell division (RND) antibiotic efflux pump

				disinfecting agents and antiseptics		
3	PDB-1	PDB1_00736 Transcriptional regulatory protein RstA	ParR	macrolide antibiotic; fluoroquinolone antibiotic; monobactam; aminoglycoside antibiotic; carbapenem; cephalosporin; cephamycin; penam; tetracycline antibiotic; phenicol antibiotic; penem; disinfecting agents and antiseptics	antibiotic efflux; reduced permeability to antibiotic	resistance-nodulation-cell division (RND) antibiotic efflux pump; Outer Membrane Porin (Opr)
4	PDB-1	PDB1_00911 Multidrug transporter	Pseudomonas aeruginosa emrE	aminoglycoside antibiotic	antibiotic efflux	small multidrug resistance (SMR) antibiotic efflux pump
5	PDB-1	PDB1_01134 Sensor protein QseC	basS	peptide antibiotic	antibiotic target alteration; antibiotic efflux	pmr phosphoethanolamine transferase
6	PDB-1	PDB1_02013 Translational regulator CsrA	rsmA	fluoroquinolone antibiotic; diaminopyrimidine antibiotic; phenicol antibiotic	antibiotic efflux	resistance-nodulation-cell division (RND) antibiotic efflux pump
7	PDB-1	PDB1_03062 Multidrug resistance protein MdtE	TriB	disinfecting agents and antiseptics	antibiotic efflux	resistance-nodulation-cell division (RND) antibiotic efflux pump

8	PDB-1	PDB1_0328 3 Multidrug resistance protein MdtK	PmpM	fluoroquinolone antibiotic; aminoglycoside antibiotic; disinfecting agents and antiseptics	antibiotic efflux	multidrug and toxic compound extrusion (MATE) transporter
9	PDB-1	PDB1_0349 9 Beta-lactamase OXA-133	OXA-847	carbapenem; cephalosporin; penam	antibiotic inactivation	OXA beta-lactamase
10	PDB-1	PDB1_0398 2 Multidrug resistance protein MexA	MexA	macrolide antibiotic; fluoroquinolone antibiotic; monobactam; carbapenem; cephalosporin; cephamycin; penam; tetracycline antibiotic; peptide antibiotic; aminocoumarin antibiotic; diaminopyrimidin e antibiotic; sulfonamide antibiotic; phenicol antibiotic; penem	antibiotic efflux	resistance-nodulation-cell division (RND) antibiotic efflux pump
11	PDB-1	PDB1_0398 4 Outer membrane protein OprM	OprM	macrolide antibiotic; fluoroquinolone antibiotic; monobactam; aminoglycoside antibiotic; carbapenem; cephalosporin; cephamycin;	antibiotic efflux	resistance-nodulation-cell division (RND) antibiotic efflux pump

				penam; tetracycline antibiotic; peptide antibiotic; aminocoumarin antibiotic; diaminopyrimidine antibiotic; sulfonamide antibiotic; phenicol antibiotic; penem; disinfecting agents and antiseptics		
12	PDB-1	PDB1_04397 Bicyclomycin resistance protein	bcr-1	bicyclomycin-like antibiotic	antibiotic efflux	major facilitator superfamily (MFS) antibiotic efflux pump
13	PDB-1	PDB1_04423 Beta-lactamase	PDC-3	monobactam; carbapenem; cephalosporin; cephamycin; penam	antibiotic inactivation	PDC beta-lactamase
14	PDB-1	PDB1_04609 Multidrug efflux pump subunit AcrB	MexW	macrolide antibiotic; fluoroquinolone antibiotic; tetracycline antibiotic; phenicol antibiotic; disinfecting agents and antiseptics	antibiotic efflux	resistance-nodulation-cell division (RND) antibiotic efflux pump
15	PDB-1	PDB1_05141 Response regulator MprA	cprR	peptide antibiotic	antibiotic target alteration; antibiotic efflux	pmr phosphoethanolamine transferase

16	PDB-1	PDB1_0516 1 Efflux pump membrane transporter BepE	MexI	fluoroquinolone antibiotic; tetracycline antibiotic; disinfecting agents and antiseptics	antibiotic efflux	resistance-nodulation-cell division (RND) antibiotic efflux pump
17	PDB-1	PDB1_0516 2 Efflux pump periplasmic linker BepF	MexH	fluoroquinolone antibiotic; tetracycline antibiotic; disinfecting agents and antiseptics	antibiotic efflux	resistance-nodulation-cell division (RND) antibiotic efflux pump
18	PDB-1	PDB1_0516 3 hypothetical protein	MexG	fluoroquinolone antibiotic; tetracycline antibiotic; disinfecting agents and antiseptics	antibiotic efflux	resistance-nodulation-cell division (RND) antibiotic efflux pump
19	PDB-1	PDB1_0541 8 Multidrug resistance protein MdtB	MuxB	macrolide antibiotic; monobactam; tetracycline antibiotic; aminocoumarin antibiotic	antibiotic efflux	resistance-nodulation-cell division (RND) antibiotic efflux pump
20	PDB-1	PDB1_0542 0 Toluene efflux pump outer membrane protein TtgF	OpmB	macrolide antibiotic; monobactam; tetracycline antibiotic; aminocoumarin antibiotic	antibiotic efflux	resistance-nodulation-cell division (RND) antibiotic efflux pump
21	PDB-1	PDB1_0545 2 Toluene efflux pump outer membrane protein TtgI	OprN	fluoroquinolone antibiotic; diaminopyrimidine antibiotic; phenicol antibiotic	antibiotic efflux	resistance-nodulation-cell division (RND) antibiotic efflux pump
22	PDB-1	PDB1_0545 3 multidrug	MexF	fluoroquinolone antibiotic;	antibiotic efflux	resistance-nodulation-cell

		efflux RND transporter permease subunit OqxB7		diaminopyrimidine antibiotic; phenicol antibiotic		division (RND) antibiotic efflux pump
23	PDB-1	PDB1_05454 Efflux pump periplasmic linker BepF	MexE	fluoroquinolone antibiotic; diaminopyrimidine antibiotic; phenicol antibiotic	antibiotic efflux	resistance-nodulation-cell division (RND) antibiotic efflux pump
24	PDB-1	PDB1_05588 Redox-sensitive transcriptional activator SoxR	Pseudomonas aeruginosa soxR	fluoroquinolone antibiotic; cephalosporin; glycylcycline; penam; tetracycline antibiotic; rifamycin antibiotic; phenicol antibiotic; disinfecting agents and antiseptics	antibiotic target alteration; antibiotic efflux	ATP-binding cassette (ABC) antibiotic efflux pump; major facilitator superfamily (MFS) antibiotic efflux pump; resistance-nodulation-cell division (RND) antibiotic efflux pump
25	PDB-1	PDB1_05899 Transcriptional regulatory protein CpxR	Pseudomonas aeruginosa CpxR	macrolide antibiotic; fluoroquinolone antibiotic; monobactam; aminoglycoside antibiotic; carbapenem; cephalosporin; cephamycin; penam; tetracycline antibiotic; peptide antibiotic; aminocoumarin antibiotic; diaminopyrimidin	antibiotic efflux	resistance-nodulation-cell division (RND) antibiotic efflux pump

				e antibiotic; sulfonamide antibiotic; phenicol antibiotic; penem		
26	PDB-2	PDB2_00298 Multidrug transporter	Pseudomonas aeruginosa emrE	aminoglycoside antibiotic	antibiotic efflux	small multidrug resistance (SMR) antibiotic efflux pump
27	PDB-2	PDB2_00521 Sensor protein QseC	basS	peptide antibiotic	antibiotic target alteration; antibiotic efflux	pmr phosphoethanolamine transferase
28	PDB-2	PDB2_00869 hypothetical protein	MexL	macrolide antibiotic; tetracycline antibiotic; disinfecting agents and antiseptics	antibiotic efflux	resistance-nodulation-cell division (RND) antibiotic efflux pump
29	PDB-2	PDB2_01017 Sec translocon accessory complex subunit YajC	YajC	fluoroquinolone antibiotic; cephalosporin; glycylcycline; penam; tetracycline antibiotic; oxazolidinone antibiotic; glycopeptide antibiotic; rifamycin antibiotic; phenicol antibiotic; disinfecting agents and antiseptics	antibiotic efflux	resistance-nodulation-cell division (RND) antibiotic efflux pump
30	PDB-2	PDB2_01834 Outer membrane	OprM	macrolide antibiotic; fluoroquinolone	antibiotic efflux	resistance-nodulation-cell division (RND)

		protein OprM		antibiotic; monobactam; aminoglycoside antibiotic; carbapenem; cephalosporin; cephamycin; penam; tetracycline antibiotic; peptide antibiotic; aminocoumarin antibiotic; diaminopyrimidine antibiotic; sulfonamide antibiotic; phenicol antibiotic; penem; disinfecting agents and antiseptics		antibiotic efflux pump
31	PDB-2	PDB2_0183 6 Multidrug resistance protein MexA	MexA	macrolide antibiotic; fluoroquinolone antibiotic; monobactam; carbapenem; cephalosporin; cephamycin; penam; tetracycline antibiotic; peptide antibiotic; aminocoumarin antibiotic; diaminopyrimidine antibiotic; sulfonamide antibiotic;	antibiotic efflux	resistance-nodulation-cell division (RND) antibiotic efflux pump

				phenicol antibiotic; penem		
32	PDB-2	PDB2_02023 Redox-sensitive transcriptional activator SoxR	Pseudomonas aeruginosa soxR	fluoroquinolone antibiotic; cephalosporin; glycylcycline; penam; tetracycline antibiotic; rifamycin antibiotic; phenicol antibiotic; disinfecting agents and antiseptics	antibiotic target alteration; antibiotic efflux	ATP-binding cassette (ABC) antibiotic efflux pump; major facilitator superfamily (MFS) antibiotic efflux pump; resistance-nodulation-cell division (RND) antibiotic efflux pump
33	PDB-2	PDB2_02804 Multidrug resistance protein MdtK	PmpM	fluoroquinolone antibiotic; aminoglycoside antibiotic; disinfecting agents and antiseptics	antibiotic efflux	multidrug and toxic compound extrusion (MATE) transporter
34	PDB-2	PDB2_03211 Response regulator MprA	cprR	peptide antibiotic	antibiotic target alteration; antibiotic efflux	pmr phosphoethanolamine transferase
35	PDB-2	PDB2_03771 Beta-lactamase OXA-133	OXA-847	carbapenem; cephalosporin; penam	antibiotic inactivation	OXA beta-lactamase
36	PDB-2	PDB2_04097 Transcriptional regulatory protein RstA	ParR	macrolide antibiotic; fluoroquinolone antibiotic; monobactam; aminoglycoside antibiotic; carbapenem; cephalosporin; cephamycin;	antibiotic efflux; reduced permeability to antibiotic	resistance-nodulation-cell division (RND) antibiotic efflux pump; Outer Membrane Porin (Opr)

				penam; tetracycline antibiotic; phenicol antibiotic; penem; disinfecting agents and antiseptics		
37	PDB-2	PDB2_04454 Beta-lactamase	PDC-3	monobactam; carbapenem; cephalosporin; cephamycin; penam	antibiotic inactivation	PDC beta-lactamase
38	PDB-2	PDB2_04480 Bicyclomycin resistance protein	bcr-1	bicyclomycin-like antibiotic	antibiotic efflux	major facilitator superfamily (MFS) antibiotic efflux pump
39	PDB-2	PDB2_04596 Translational regulator CsrA	rsmA	fluoroquinolone antibiotic; diaminopyrimidine antibiotic; phenicol antibiotic	antibiotic efflux	resistance-nodulation-cell division (RND) antibiotic efflux pump
40	PDB-2	PDB2_04771 Multidrug resistance protein MdtE	TriB	disinfecting agents and antiseptics	antibiotic efflux	resistance-nodulation-cell division (RND) antibiotic efflux pump
41	PDB-2	PDB2_05136 hypothetical protein	MexG	fluoroquinolone antibiotic; tetracycline antibiotic; disinfecting agents and antiseptics	antibiotic efflux	resistance-nodulation-cell division (RND) antibiotic efflux pump
42	PDB-2	PDB2_05137 Efflux pump periplasmic linker BepF	MexH	fluoroquinolone antibiotic; tetracycline antibiotic; disinfecting agents and antiseptics	antibiotic efflux	resistance-nodulation-cell division (RND) antibiotic efflux pump

43	PDB-2	PDB2_05138 Efflux pump membrane transporter BepE	MexI	fluoroquinolone antibiotic; tetracycline antibiotic; disinfecting agents and antiseptics	antibiotic efflux	resistance-nodulation-cell division (RND) antibiotic efflux pump
44	PDB-2	PDB2_05350 Multidrug resistance protein MdtB	MuxB	macrolide antibiotic; monobactam; tetracycline antibiotic; aminocoumarin antibiotic	antibiotic efflux	resistance-nodulation-cell division (RND) antibiotic efflux pump
45	PDB-2	PDB2_05352 Toluene efflux pump outer membrane protein TtgF	OpmB	macrolide antibiotic; monobactam; tetracycline antibiotic; aminocoumarin antibiotic	antibiotic efflux	resistance-nodulation-cell division (RND) antibiotic efflux pump
46	PDB-2	PDB2_05384 Toluene efflux pump outer membrane protein TtgI	OprN	fluoroquinolone antibiotic; diaminopyrimidine antibiotic; phenicol antibiotic	antibiotic efflux	resistance-nodulation-cell division (RND) antibiotic efflux pump
47	PDB-2	PDB2_05385 multidrug efflux RND transporter permease subunit OqxB7	MexF	fluoroquinolone antibiotic; diaminopyrimidine antibiotic; phenicol antibiotic	antibiotic efflux	resistance-nodulation-cell division (RND) antibiotic efflux pump
48	PDB-2	PDB2_05386 Efflux pump periplasmic linker BepF	MexE	fluoroquinolone antibiotic; diaminopyrimidine antibiotic; phenicol antibiotic	antibiotic efflux	resistance-nodulation-cell division (RND) antibiotic efflux pump

49	PDB-2	PDB2_05842 Transcriptional regulatory protein CpxR	Pseudomonas aeruginosa CpxR	macrolide antibiotic; fluoroquinolone antibiotic; monobactam; aminoglycoside antibiotic; carbapenem; cephalosporin; cephamycin; penam; tetracycline antibiotic; peptide antibiotic; aminocoumarin antibiotic; diaminopyrimidine antibiotic; sulfonamide antibiotic; phenicol antibiotic; penem	antibiotic efflux	resistance-nodulation-cell division (RND) antibiotic efflux pump

Table 4: Virulence Factors identified in isolates PDB-1 and PDB-2, as determined by Vfanalyzer

VFclass	Virulence factors	Related genes	PDB-1(Prediction)	PDB-2(Prediction)
			draft (draft)	draft (draft)
Adherence	Flagella	flaG	PDB1_02319	PDB2_01453
		fleN	PDB1_03205	PDB2_02883
		fleQ	PDB1_02315	PDB2_01457
		fleR	PDB1_02313	PDB2_01459
		fleS	PDB1_02314	PDB2_01458
		flgA	PDB1_05071	PDB2_03490
		flgB	PDB1_02335	PDB2_01437
		flgC	PDB1_02334	PDB2_01438
		flgD	PDB1_02333	PDB2_01439
		flgE	PDB1_02332	PDB2_01440
		flgF	PDB1_02331	PDB2_01441
		flgG	PDB1_02330	PDB2_01442
		flgH	PDB1_02329	PDB2_01443
		flgI	PDB1_02328	PDB2_01444
		flgJ	PDB1_02327	PDB2_01445
		flgK	PDB1_02326	PDB2_01446
		flgL	PDB1_02325	PDB2_01447
		flgM	PDB1_05070	PDB2_03491
		flgN	PDB1_05069	PDB2_03492
		flhA	PDB1_03207	PDB2_02881
		flhB	PDB1_03210	PDB2_02878
		flhF	PDB1_03206	PDB2_02882
		fliA	PDB1_03204	PDB2_02884
		fliC	PDB1_02320	PDB2_01452
		fliD	PDB1_02318	PDB2_01454
		fliE	PDB1_02312	PDB2_01460
		fliF	PDB1_02311	PDB2_01461
		fliG	PDB1_02310	PDB2_01462
		fliH	PDB1_02309	PDB2_01463
		fliI	PDB1_02308	PDB2_01464
		fliJ	PDB1_02307	PDB2_01465
		fliK	PDB1_03218	PDB2_02870
		fliL	PDB1_03217	PDB2_02871
		fliM	PDB1_03216	PDB2_02872
		fliN	PDB1_03215	PDB2_02873
		fliO	PDB1_03214	PDB2_02874
		fliP	PDB1_03213	PDB2_02875
		fliQ	PDB1_03212	PDB2_02876
		fliR	PDB1_03211	PDB2_02877
		fliS	PDB1_02317	PDB2_01455
		fliT	PDB1_02316	PDB2_01456
		motA	PDB1_00949	PDB2_00336
		motB	PDB1_00950	PDB2_00337
		motC	PDB1_03199	PDB2_02889
		motD	PDB1_03198	PDB2_02890
		motY	PDB1_04096	PDB2_00714

	LPS O-antigen (P. aeruginosa)	Undetermined	PDB1_05946; PDB1_05949; PDB1_05954; PDB1_05960; PDB1_05961	PDB2_05889; PDB2_05892; PDB2_05897; PDB2_05903; PDB2_05904
	Type IV pili biosynthesis	fimT	-	-
		fimU	PDB1_02633	PDB2_04284
		fimV	PDB1_05993	PDB2_05932
		pilA	-	-
		pilB	PDB1_02605	PDB2_04256
		pilC	PDB1_02606	PDB2_04257
		pilD	PDB1_02607	PDB2_04258
		pilE	PDB1_02639	PDB2_04290
		pilF	PDB1_00212	PDB2_01000
		pilM	PDB1_00856	PDB2_00243
		pilN	PDB1_00857	PDB2_00244
		pilO	PDB1_00858	PDB2_00245
		pilP	PDB1_00859	PDB2_00246
		pilQ	PDB1_00860	PDB2_00247
		pilR	PDB1_02630	PDB2_04281
		pilS	PDB1_02629	PDB2_04280
		pilT	PDB1_03952	PDB2_01866
		pilU	PDB1_03953	PDB2_01865
		pilV	PDB1_02634	PDB2_04285
		pilW	PDB1_02635	PDB2_04286
		pilX	PDB1_02636	PDB2_04287
		pilY1	PDB1_02637	PDB2_04288
		pilY2	-	-
		pilZ	PDB1_01586	PDB2_03331
	Type IV pili twitching motility related proteins	chpA	PDB1_03970	PDB2_01848
		chpB	PDB1_03971	PDB2_01847
		chpC	PDB1_03972	PDB2_01846
		chpD	PDB1_03973	PDB2_01845
		chpE	PDB1_03974	PDB2_01844
		pilG	PDB1_03965	PDB2_01853
		pilH	PDB1_03966	PDB2_01852
		pilI	PDB1_03967	PDB2_01851
		pilJ	PDB1_03968	PDB2_01850
		pilK	PDB1_03969	PDB2_01849
Antimicrobial activity	Phenazines biosynthesis	phzA1	-	-
		phzA2	PDB1_00843	PDB2_05270
		phzB1	-	-
		phzB2	PDB1_00844	PDB2_05271
		phzC1	PDB1_05736	PDB2_05733
		phzC2	-	-
		phzD1	PDB1_05733	PDB2_05730
		phzD2	-	-
		phzE1	-	PDB2_04905
		phzE2	-	-
		phzF1	PDB1_04872	PDB2_04906
		phzF2	-	-
		phzG1	-	-
		phzG2	PDB1_04871	PDB2_04907

		phzH	PDB1_03167	PDB2_04688
		phzM	PDB1_05159	PDB2_05140
		phzS	PDB1_05295	PDB2_05344
Antiphagocytosis	Alginate biosynthesis	alg44	PDB1_04112	PDB2_00730
		alg8	PDB1_04111	PDB2_00729
		algA	PDB1_04121	PDB2_00739
		algC	PDB1_04743	PDB2_04857
		algD	PDB1_04110	PDB2_00728
		algE	PDB1_04114	PDB2_00732
		algF	PDB1_04120	PDB2_00738
		algG	PDB1_04115	PDB2_00733
		algI	PDB1_04118	PDB2_00736
		algJ	PDB1_04119	PDB2_00737
		algK	PDB1_04113	PDB2_00731
		algL	PDB1_04117	PDB2_00735
		algX	PDB1_04116	PDB2_00734
	Alginate regulation	algP/algR3	PDB1_04184	PDB2_00021
		algQ	PDB1_04182	PDB2_00019
		algR	PDB1_04176	PDB2_00013
		algU	PDB1_02157	PDB2_02690
		algW	PDB1_02522	PDB2_03118
		algZ	PDB1_04175	PDB2_00012
		mucA	PDB1_02156	PDB2_02689
		mucB	PDB1_02155	PDB2_02688
		mucC	PDB1_02154	PDB2_02687
		mucD	PDB1_02153	PDB2_02686
		mucE	PDB1_04503	PDB2_04374
		mucP	PDB1_00051	PDB2_00839
	Capsular polysaccharide(Vibrio)	wcaJ	PDB1_05957	PDB2_05900
Biosurfactant	Rhamnolipid biosynthesis	rhlA	PDB1_04069	PDB2_00687
		rhlB	PDB1_04068	PDB2_00686
		rhlC	PDB1_02280	PDB2_01492
Enzyme	Hemolytic phospholipase C	plcH	PDB1_02076	PDB2_04533
	Non-hemolytic phospholipase C	plcN	PDB1_04381	PDB2_03458
	Phospholipase C	plcB	PDB1_03582	PDB2_04792
	Phospholipase D	pldA	-	-
Iron uptake	Achromobactin biosynthesis and transport	acsA	-	-
		acsB	-	-
		acsC	-	-
		acsD	-	-
		cbrA	-	-
		cbrB	-	-
		cbrC	-	-
		cbrD	-	-
	Pyochelin receptor	fptA	PDB1_05291	PDB2_05340
	Pyochelin	pchA	PDB1_05281	PDB2_05329
		pchB	PDB1_05282	PDB2_05330
		pchC	PDB1_05283	PDB2_05331
		pchD	PDB1_05284	PDB2_05332

		pchE	PDB1_05286	PDB2_05334
		pchF	PDB1_05287	PDB2_05335
		pchG	PDB1_05288	PDB2_05336
		pchH	PDB1_05289	PDB2_05337; PDB2_05338
		pchI	PDB1_05290	PDB2_05339
		pchR	PDB1_05285	PDB2_05333
	Pyoverdine receptors	fpvA	PDB1_04612	PDB2_03630
	Pyoverdine	pvdA	PDB1_04625	PDB2_03618
		pvdD	-	-
		pvdE	PDB1_04613	PDB2_03629
		pvdF	PDB1_04614	PDB2_03628
		pvdG	PDB1_04908	PDB2_03657
		pvdH	PDB1_04921	PDB2_03644
		pvdI	PDB1_05713	PDB2_03632; PDB2_03633
		pvdJ	PDB1_04611	PDB2_03631
		pvdL	PDB1_04909	PDB2_03656
		pvdM	PDB1_04617	PDB2_03625
		pvdN	PDB1_04616	PDB2_03626
		pvdO	PDB1_04615	PDB2_03627
		pvdP	PDB1_04618	PDB2_03624
		pvdQ	PDB1_04626	PDB2_03617
		pvdS	PDB1_04907	PDB2_03658
		pvdY	PDB1_04906	PDB2_03659
	Yersiniabactin	fyuA	-	-
		irp1	-	-
		irp2	-	-
		irp3	-	-
		irp4	-	-
		irp5	-	-
		ybtA	-	-
		ybtP	-	-
		ybtQ	-	-
Protease	Alkaline protease	aprA	PDB1_05681	PDB2_05699
	Elastase	lasA	PDB1_00813	PDB2_05240
		lasB	PDB1_00126	PDB2_00914
	Protease IV	prpL	PDB1_05193	PDB2_05106
Quorum sensing	Acylhomoserine lactone synthase	hdtS	PDB1_03561	PDB2_03709
	N-(3-oxo-dodecanoyl)-L-homoserine lactone QS system	lasI	PDB1_03227	PDB2_02861
		lasR	PDB1_03230	PDB2_02858
	N-(3-oxo-hexanoyl)-Lhomoserine lactone QS system	ahlI	-	-
		ahlR	-	-
	N-(butanoyl)-L-homoserine lactone QS system	rhlI	PDB1_04066	PDB2_00684
		rhlR	PDB1_04067	PDB2_00685
Regulation	GacS/GacA two-component system	gacA	PDB1_02901	PDB2_03003
		gacS	PDB1_01987	PDB2_01189
	Harpins	hopP1	-	-

Secretion system		hrpA1	-	-
		hrpA2	-	-
		hrpK1	-	-
		hrpW1	-	-
		hrpZ1	-	-
	Hcp secretion island-1 encoded type VI secretion system (H-T6SS)	Undetermined	PDB1_03148	PDB2_04669
		Undetermined	PDB1_03147	PDB2_04668
		Undetermined	PDB1_03146	PDB2_04667
		Undetermined	PDB1_03143	PDB2_04664
		Undetermined	PDB1_03141	PDB2_04662
		Undetermined	PDB1_03140	PDB2_04661
		Undetermined	PDB1_03139	PDB2_04660
		Undetermined	PDB1_03137	PDB2_04658
		Undetermined	PDB1_03136	PDB2_04657
		Undetermined	PDB1_03135	PDB2_04656
		Undetermined	PDB1_03133	PDB2_04654
		Undetermined	PDB1_03132	PDB2_04653
		Undetermined	PDB1_03131	PDB2_04652
		Undetermined	PDB1_03130	PDB2_04651
		clpV1	PDB1_03129	PDB2_04650
		fha1	PDB1_03138	PDB2_04659
		hcp1	PDB1_03134	PDB2_04655
		icmF1	PDB1_03142	PDB2_04663
		ppkA	PDB1_03145	PDB2_04666
		pppA	PDB1_03144	PDB2_04665
		vgrG1	PDB1_02797; PDB1_02798; PDB1_03124; PDB1_03128	PDB2_02615; PDB2_02616; PDB2_04645; PDB2_04649
	P. aeruginosa TTSS translocated effectors	exoS	PDB1_00251	PDB2_01038
		exoT	PDB1_03175	PDB2_04696
		exoU	-	-
		exoY	PDB1_01291	PDB2_02105
	P. aeruginosa TTSS	exsA	PDB1_00641	PDB2_04192
		exsB	PDB1_00640	PDB2_04193
		exsC	PDB1_00638	PDB2_04195
		exsD	PDB1_00642	PDB2_04191
		exsE	PDB1_00639	PDB2_04194
		pcr1	PDB1_00627	PDB2_04206
		pcr2	PDB1_00628	PDB2_04205
		pcr3	PDB1_00629	PDB2_04204
		pcr4	PDB1_00630	PDB2_04203
		pcrD	PDB1_00631	PDB2_04202
		pcrG	PDB1_00633	PDB2_04200
		pcrH	PDB1_00635	PDB2_04198
		pcrR	PDB1_00632	PDB2_04201
		pcrV	PDB1_00634	PDB2_04199
		popB	PDB1_00636	PDB2_04197
		popD	PDB1_00637	PDB2_04196
		popN	PDB1_00626	PDB2_04207
		pscB	PDB1_00643	PDB2_04190
		pscC	PDB1_00644	PDB2_04189
		pscD	PDB1_00645	PDB2_04188

		pscE	PDB1_00646	PDB2_04187
		pscF	PDB1_00647	PDB2_04186
		pscG	PDB1_00648	PDB2_04185
		pscH	PDB1_00649	PDB2_04184
		pscI	PDB1_00650	PDB2_04183
		pscJ	PDB1_00651	PDB2_04182
		pscK	PDB1_00652	PDB2_04181
		pscL	PDB1_00653	PDB2_04180
		pscN	PDB1_00625	PDB2_04208
		pscO	PDB1_00624	PDB2_04209
		pscP	PDB1_00623	PDB2_04210
		pscQ	PDB1_00622	PDB2_04211
		pscR	PDB1_00621	PDB2_04212
		pscS	PDB1_00620	PDB2_04213
		pscT	PDB1_00619	PDB2_04214
		pscU	PDB1_00618	PDB2_04215
	P. syringae TTSS effectors	avrB2	-	-
		avrB3	-	-
		avrB4-1	-	-
		avrB4-2	-	-
		avrD1	-	-
		avrE1	-	-
		avrPto1	-	-
		avrRpm1	-	-
		avrRps4	-	-
		hopA1	-	-
		hopAA1'	-	-
		hopAA1-1	-	-
		hopAA1-2	-	-
		hopAA1	-	-
		hopAB1	-	-
		hopAB2	-	-
		hopAB3'	-	-
		hopAC1	-	-
		hopAC	-	-
		hopAD1	-	-
		hopAE1	-	-
		hopAF1	-	-
		hopAG1	-	-
		hopAG	-	-
		hopAH1	-	-
		hopAH2-1	-	-
		hopAH2-2	-	-
		hopAH2	-	-
		hopAI1'	-	-
		hopAI1	-	-
		hopAJ1	-	-
		hopAJ2	-	-
		hopAK1	-	-
		hopAM1-1	-	-
		hopAM1-2	-	-
		hopAN1	-	-

		hopAO1	-	-
		hopAP1	-	-
		hopAQ1	-	-
		hopAS1'	-	-
		hopAS1	-	-
		hopAT1'	-	-
		hopAT1	-	-
		hopAU1	-	-
		hopAV1	-	-
		hopAW1	-	-
		hopB1	-	-
		hopC1	-	-
		hopD1	-	-
		hopD	-	-
		hopE1	-	-
		hopF2	-	-
		hopF3	-	-
		hopG1	-	-
		hopH1	-	-
		hopI1	-	-
		hopJ1	-	-
		hopK1	-	-
		hopL1	-	-
		hopM1'	-	-
		hopM1	-	-
		hopN1	-	-
		hopO1-1	-	-
		hopO1-3'	-	-
		hopP1-2	-	-
		hopQ1-1	-	-
		hopQ1-2	-	-
		hopQ1	-	-
		hopR1	-	-
		hopS1'	-	-
		hopS2	-	-
		hopT1-1	-	-
		hopT1-2	-	-
		hopT2	-	-
		hopU1	-	-
		hopV1	-	-
		hopW1-1	-	-
		hopW1-2	-	-
		hopX1	-	-
		hopY1	-	-
		hopZ3	-	-
	P. syringae TTSS	hrcC	-	-
		hrcJ	-	-
		hrcN	-	-
		hrcQa	-	-
		hrcQb	-	-
		hrcR	-	-
		hrcS	-	-

		hrcT	-	-
		hrcU	-	-
		hrcV	-	-
		hrpB	-	-
		hrpD	-	-
		hrpE	-	-
		hrpF	-	-
		hrpG	-	-
		hrpJ	-	-
		hrpL	-	-
		hrpO	-	-
		hrpP	-	-
		hrpQ	-	-
		hrpR	-	-
		hrpS	-	-
		hrpT	-	-
		hrpV	-	-
		shcA	-	-
		shcE	-	-
		shcF	-	-
		shcM	-	-
		shcN	-	-
		shcS1	-	-
		shcS2	-	-
		shcV	-	-
Toxin	Exolysin	exlA	-	-
		exlB	-	-
	Exotoxin A (ETA)	toxA	PDB1_02261	PDB2_01511
	Hydrogen cyanide production	hcnA	PDB1_01289	PDB2_02103
		hcnB	PDB1_01288	PDB2_02102
		hcnC	PDB1_01287	PDB2_02101
	Phytotoxin coronatine	Undetermined	-	-
		cfa1	-	-
		cfa2	-	-
		cfa3	-	-
		cfa4	-	-
		cfa5	-	-
		cfa6	-	-
		cfa7	-	-
		cfa8	-	-
		cfa9	-	-
		cfl	-	-
		cmaA	-	-
		cmaB	-	-
		cmaC	-	-
		cmaD	-	-
		cmaE	-	-
		cmaT	-	-
		cmaU	-	-
		corP	-	-
		corR	-	-
		Undetermined	-	-

	Phytotoxin phaseolotoxin	Undetermined	-	-
		Undetermined	-	-
		Undetermined	-	-
		Undetermined	-	-
		Undetermined	-	-
		Undetermined	-	-
		Undetermined	-	-
		Undetermined	-	-
		Undetermined	-	-
		Undetermined	-	-
		Undetermined	-	-
		Undetermined	-	-
		Undetermined	-	-
		Undetermined	-	-
		Undetermined	-	-
		Undetermined	-	-
		argD	-	-
		argK	-	-
		cysC1	-	-
		dcd2	-	-
	Phytotoxin syringomycin	syrB1	-	-
		syrB2	-	-
		syrC	-	-
		syrD	-	-
		syrE	-	-
		syrF	-	-
		syrP	-	-
	Phytotoxin syringopeptin	sypA	-	-
		sypB	-	-
		sypC	-	-
	TccC-type insecticidal toxins	Undetermined	-	-
Immune evasion	Capsule(Acinetobacter)		PDB1_02268	PDB2_01504

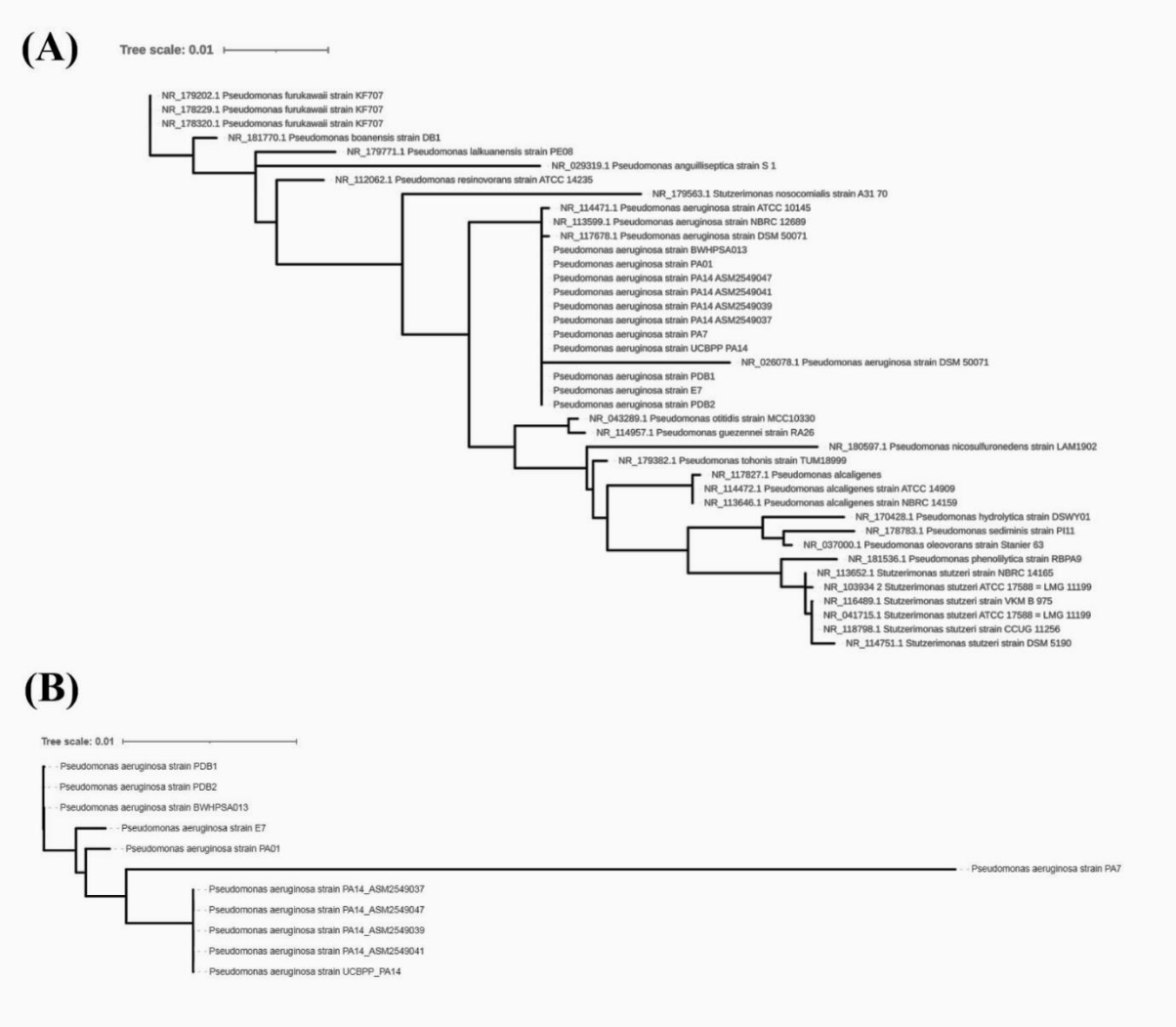

Figure 11: Phylogenetic analysis of the isolated strains. (A) Tree built from 16S rRNA sequences of the isolates PDB1 and PDB2, other *P. aeruginosa* strains, and closely aligned 16S rRNA sequences. (B) Tree built from the core gene alignment among PDB1, PDB2, and other *P. aeruginosa* strains used for the pan-genome analysis

3.7 Biosurfactant Assay

Both the oil spread test and drop collapse test showed positive biosurfactant activity. For the oil spread test, all the systems except negative control showed dispersion upon interaction. When mixed, the systems with biosurfactant produced oil-water emulsion comparable to positive control. (Figure 12)

On the other hand, for the drop collapse test, negative control and system 9 which was the 1-year-old bacteria in MSB had a round-shaped drop. However, system 9 gave mixed results as one part was flat and one part was round shape (Figure 13)

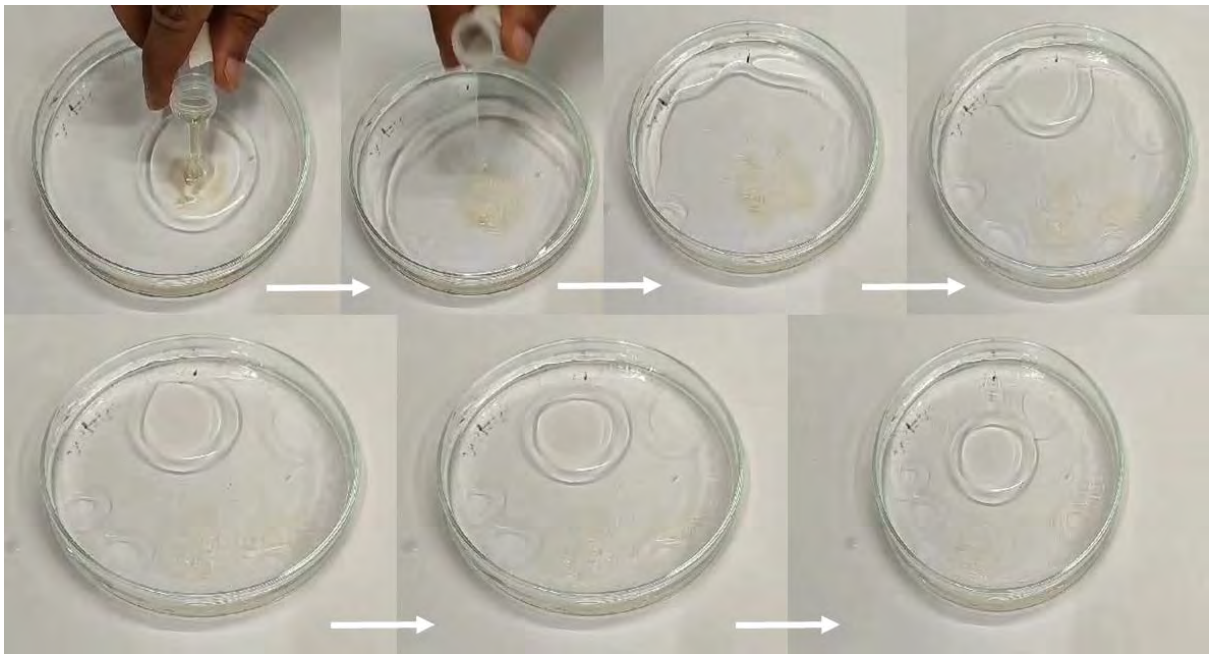

Figure 12: Oil spread test. As a continuous steps, it was shown when cell free supernatant interacts with oil, it disperses the oil and make a zone proving biosurfactant activity

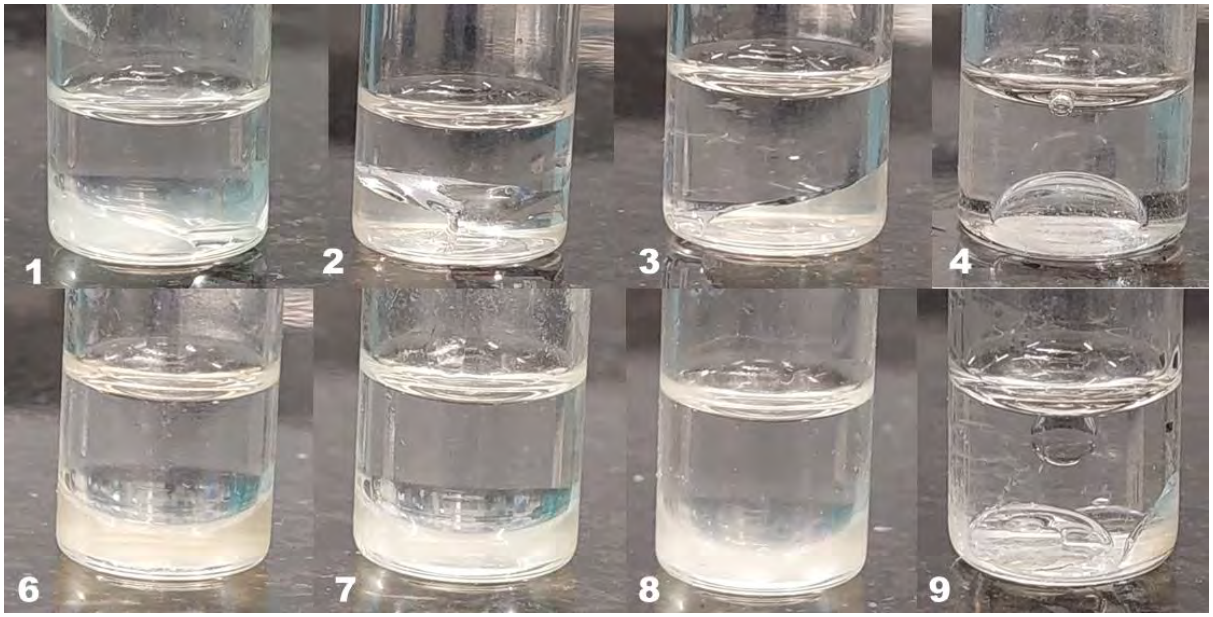

Figure 13: Drop collapse test. 1. Nutrient broth inoculated with bacteria. 2. Nutrient broth inoculated with bacteria and added soybean oil. 3. Nutrient broth inoculated with bacteria added paraffin oil. 4. Nutrient broth (Negative control). 6. 4-month-old bacteria culture+ Nutrient broth+ soybean oil. 7. 4-month-old bacteria culture+ Nutrient broth+ paraffin oil. 8. 4-month-old bacteria culture. 9. 1-Year-old bacteria culture with mixed result

3.8 AST Analysis

According to the perfect matches with antibiotic-resistant genes, 7 different classes of antibiotics were chosen. Tetracycline 30 mg (tetracycline class), ampicillin 10mg (penicillin class), erythromycin 15 mg (macrolide class), ceftazidime 30 mcg (third-generation cephalosporin), tigercycline 15 mcg (glycylcycline class), kanamycin 5mcg (aminoglycoside class) and Meropenem+ EDTA (carbapenem class) were chosen as representatives.

Both PDB-1 and PDB-2 were found to be resistant to all the listed antibiotics. For PDB-1, a small zone can be observed for tetracycline, kanamycin, and tigercycline though they were all less than the required zone diameter for them to be susceptible. The same result was observed for PDB-2. (Figure)

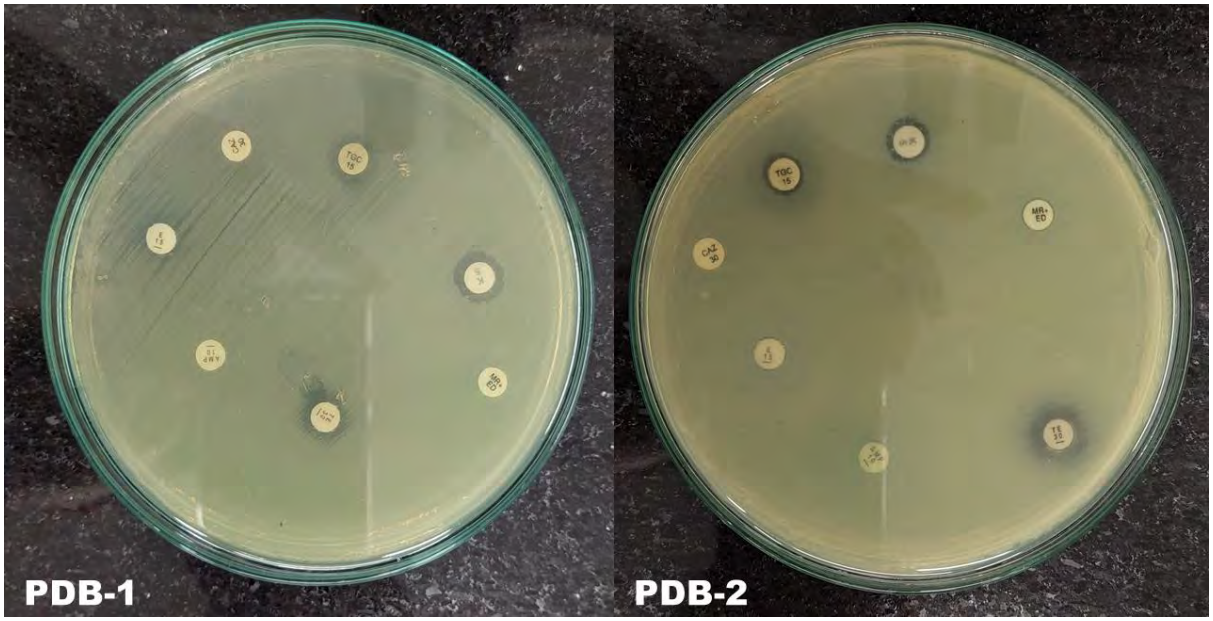

Figure 14: AST analysis of PDB-1 and PDB-2. Both bacteria were resistant to seven class of antibiotics as seen from WGS analysis

Chapter 4

Discussion

This study has proved the biodegradation capability of *Zophobas atratus* larvae and its gut bacteria. In this study, larvae ate 15.12% LLDPE, 24.04% LDPE, and 20.01% EPS in 36 days with respective survival rates of 87% ± 10.4%, 85% ± 10%, 90% ± 8.66% with brown particle-like frass excreting in every system. This result is comparable to the other studies done on the same larvae, for example (Peng et al., 2020) had almost the same PC and SR for LDPE. the small difference between SR and PC may lie in the absence of any controlled temperature and humidity in this study. For EPS, the outcome is comparable to the study by (Yang et al., 2020). The SR values show that larvae can survive with EPS better than the other two types, but they can consume LDPE at a much higher rate than the others. For the frass and cannibalism, other studies also reported the same results and the frass structure was distinct.

For all the groups except the PCN, the LW decreased over time, similar to the observations of (Luo et al., 2021). When compared with PCN LW, significant change can be observed from 36 days onwards for LDPE and EPS and from 24 days onwards for LLDPE. Though there is no significant difference in LW decrease among the three plastic types, a decrease in weight when compared with SR suggests that the larvae can only survive by eating only plastic, not flourish. This result also confirms why even after molting, LW decreased. The LW values are more dissimilar when compared to other studies. Though cannibalism was observed in the system, the SR for NCN was much lower than the others. So, even if cannibalism occurred, it provided inefficient nutrition which contributed to higher larvae mortality. On the other hand, those larvae who consumed plastic had better nutrition and survived at a higher rate. In the LW graph, NCN consistently showed the lowest value. This signifies the lower growth rate of the larvae when plastic feed was absent. In combination, the lower SR and LW values when plastic feed was absent prove that the polymers provided nutrition alongside cannibalism to the larvae. One

of the aims of the experiments was to see how the larvae can degrade plastics when exposed to high temperatures and humidity. This is the expected environmental condition when performing in situ bioremediation in Bangladesh and similar tropical locations. Hence they were not placed in an incubator and had to cope with high (41ºC) to moderate temperatures with varying humidity. This unique condition may explain the differences in observations with other studies that used insect incubators.

Furthermore, FTIR analysis proved the formation of new functional groups. As stated earlier, for all the plastic types, control plastic, consumed plastic, and frass were analyzed. The data was compared among these three types and the main new functional groups that were identified were at 1075-1150 cm^{-1} (-C-O stretch), 1700 cm^{-1} (-C=O stretch), and 3440 cm^{-1} (Re-OH stretch) wavenumbers, a similar observation to Peng *et al.*, (2020)**.** These functional groups indicate oxidation of the ingested LDPE, LLDPE, and EPS in the larval gut. For all three plastic types, these three functional groups were found in the frass whereas control and consumed plastics had almost similar results. According to previous studies, the incorporation of oxygen functional groups is considered the preliminary and important step towards plastic degradation (Gautam et al., 2007; Shah et al., 2008). Findings of these groups in the frass indicate plastic metabolism/degradation.

As the frass collected was produced by the larvae by eating only plastics, it is evident that some change in the plastic structure was made during consumption. If these larvae could secrete plastic-degrading enzymes like *Galleria mellonella,* FTIR analysis would have found a difference between the control plastic and consumed plastic (Sanluis-Verdes et al., 2022). As for all the plastic types, control and consumed plastics showed nearly the same data, it can be said that the oxidation must be done during digestion. The 1700 cm^{-1} peak in consumed LDPE can be a false positive data. Previous studies confirmed that when the gut microbiome of the larvae was inhibited by antibiotics, the plastic degradation capability was also inhibited (Peng

et al., 2020; Yang et al., 2020). As a result, this oxidation is more likely caused by the gut microbiome. The frass had residual plastics, which also means they could not fully degrade the plastic that they consume.

For bacterial growth, as *P. aeruginosa* was the target bacteria, spread plating was carried out after incubation was complete with the mediums, NA, MacConkey agar, and Cetrimide agar. Colony growth on Cetrimide agar was chosen for further analysis, as it is used for the selective isolation of *Pseudomonas,* the target bacteria (Brown & Lowbury, 1965). Using this media also enhances the production of *Pseudomonas* pigments pyocyanin and pyoverdine, which show a characteristic blue-green and yellow-green color respectively. This aided the pigmentation analysis required for differentiation using colony morphology. As bacteria from all three systems (LDPE-, LLDPE-, and EPS-supplemented media) could grow on Cetrimide agar, whereas no bacteria were visible from PCB and NCB, this proves that without a carbon source, those frass bacteria cannot survive for more than 7 days. Even if there is an additional carbon source such as glucose, it is limiting; after glucose gets depleted, bacteria die. On the other hand, as long as plastics are available as carbon sources, the bacteria survive.

From the SEM analysis, it was proven that both PDB-1 and PDB-2 can degrade plastics as they showed surface degradation under SEM when compared with controls. After two months of incubation, all plastics showed surface degradation; control samples had smooth surfaces, whereas rough, broken surfaces with bacteria and biofilms could be seen in the incubated ones. The LDPE results are comparable to a previous study by (Khandare et al., 2021). The degradation pattern of LLDPE is similar to the study by (Shabbir et al., 2020).

The WGS results were analyzed with different *P. aeruginosa* strains along with analyzing differences between PDB-1 and PDb-2. Differentiation between PDB-1 and PDB-2 and comparison with other strains previously mentioned was based on sequence similarity among the annotated proteins. Strains were chosen with specific characteristics to make an informed

decision on the categorization of the isolated strains. PE-degrading strain E7, and LDPE-degrading strain PA01 as well as biosurfactant-producing strains UCBPP-PA14 and PA7 were chosen to understand how close the isolated strains are to these known plastic-degrading *P. aeruginosa* strains. Highly virulent PA14 strains were also chosen to find a distinction between plastic-degrading and virulent strains. Now, in this study, plastic degrading enzymatic pathways were searched from the WGS data to see if known enzymes and enzymatic pathways were available. For the polyethylene degrading enzymatic pathway, Yeom *et al.*, (2022) proposed a cytochrome P450 (P450)-driven cascade which starts with microbial deterioration of PE into alkane and is followed by hydroxylation by a hypothetical hydroxylase that may include P450. Then alcohol dehydrogenase, Baeyer-Villiger monooxygenase, and esterase work sequentially to produce alcohol and acid. From the sequences of this study, Cytochrome P450 107B1 gene, with P450-driven monooxygenase activity was found along with short-chain dehydrogenase, esterase, and Baeyer-Villiger monooxygenase respectively residing in the same operon. On the other hand, short-chain alcohol dehydrogenase and Baeyer-Villiger monooxygenase belonging to another operon were also found. Both of these operons seem suited for performing part of the degradation pathway. Additionally, alcohol dehydrogenases (*adh*) gene was also found which means most of the enzymes required in the pathway were present. Moreover, Cu-binding laccases, which are multi-copper oxidases, are predicted to be involved in the PE degradation pathway, as observed in previous studies (Fujisawa et al., 2001; Santo et al., 2013) and this enzyme was also present. Another enzyme, alkane hydroxylase or alkane monooxygenase (*alkB)* is also reported to be involved in PE degradation (Jeon & Kim, 2015) and genes for these enzymes were also found within the sequence.

When comparing these genes with other PE-degrading strains, orthologs were identified in most cases with over 99% sequence similarity. However, for PDB1_01395 and PDB1_01294, orthologs were not found in E7. Specifically, PDB1_01395 matched only with orthologs from

PDB-2, PA01, and BWHPSA013, while PDB1_01294 matched only with orthologs from PDB-2 and PA01. This exclusivity may suggest a specific function for PE degradation performed by these enzymes, absent in other strains. The annotation of the PA7 strain identified a dye-decolorizing peroxidase (yfeX), corresponding to the protein PSPA7_2468 (GenBank Accession: ABR83505), previously labeled as a hypothetical protein. YfeX protein is associated with lignin peroxidases, which are predicted to be involved in the PE-degrading pathway (Mukherjee & Kundu, 2014). Unfortunately, there were no orthologous sequences of YfeX present in the isolated samples.

For EPS degradation, cleavage of the main chain can lead to styrene, which can then be broken down through two different metabolic pathways (Hou & Majumder, 2021). One of these requires styrene monooxygenase, and the other requires styrene dioxygenase. According to the Biocatalysis/Biodegradation Database (BBD) (Gao et al., 2010), in *Pseudomonas,* styrene monooxygenase, styrene oxide isomerase, and phenylacetaldehyde dehydrogenase work sequentially to convert styrene to phenylacetaldehyde, which is then passed on to the phenylacetate pathway. From the sequence, a short protein sequence annotated as phenylacetaldehyde dehydrogenase (*styD)* was found, but the coded protein was too short to be independently functional. For EPS degradation, it is known that polystyrene is a vinyl polymer and phenylacetaldehyde dehydrogenase is one of the most important enzymes to metabolize vinyl groups (Danso et al., 2019; Kiel et al., 2022). No genes were annotated as styrene monooxygenase and styrene oxide isomerase in this genome, nor could any be identified from the BLASTKoala search. P450 monooxygenases and alkane hydroxylases are also probable candidates to break the main-chain C-C bonds of PS, while the side-chain is perhaps cleaved by ring-hydroxylating dioxygenases (Hou & Majumder, 2021). According to previous studies, homoserine dehydrogenase (*hom*) and S-formylglutathione hydrolase (*yeiG*) genes also participate in plastic degradation, which is present in these isolates (H. R. Kim et

al., 2020; H.-W. Kim et al., 2021). Other studies show that monooxygenases, alcohol dehydrogenases, and aldehyde dehydrogenases, all present in both strains, work together while degrading PE or PE-type plastics via an Oxo-degradation system (Gautam et al., 2007; Zeenat et al., 2021).

As previously mentioned there were several antibiotic-resistant genes were found, and they were in the bacterial chromosome. To prove they are expressed, AST was performed and showed the same result according to CLSI guidelines. Antibiotic resistance poses a problem while doing bioremediation, especially when *in situ*, as it increases the probability of transferring antibiotic resistance genes to other susceptible bacteria. However, plastic biodegradation can be more efficient with *ex-situ* methods, which will decrease the chance of spreading antibiotic resistance genes.

Virulence factors that are present in the isolates were analyzed and compared with other strains, and an important pathway involved in the production of rhamnolipid, a biosurfactant, was identified. Rhamnolipid is already in use for oil recovery, especially petroleum oils (Al-Sakkaf & Onaizi, 2023; Wei et al., 2020; Yan et al., 2012). Rhamnolipid biosynthesis has three genes, *rhlA, rhlB,* and *rhlC* (Toribio et al., 2010), and both isolates had all three genes. To prove these genes are expressed, biosurfactant assay was performed and all the systems had produced the rhamnolipid comparable to 10% Triton X-100. This result emphasizes the importance of these isolates in bioremediation, as they have potential utility for environmental recovery during oil spills.

As discussed earlier, PDB-1 isolate was identified from LDPE- and LLDPE-supplemented media, whereas PDB-2 isolate was sourced from EPS-supplemented media. However, it was not experimentally determined whether PDB-1 can grow on EPS and vice versa. MLST typing as well as comparison between protein sequences indicate that both isolates are

phylogenetically not very distinct. In the future, further experiments may show that both strains are capable of degrading all three types of plastics.

Conclusion

Zophobus atratus larvae successfully survived on three different types of plastic, LDPE, LLDPE, and EPS, with varying rates of plastic degradation and survivability. FTIR analysis showed plastic oxidation occurring at the larval gut, indicating the gut microbiome was responsible. When bacteria isolated from the larval frass were cultured with plastics as the sole carbon source, growth was observed while SEM analysis (of the plastic samples incubated with isolated bacteria) confirmed the role of bacteria in plastics degradation. The isolated bacteria were later identified as *P. aeruginosa* and extensively characterized by whole genome sequencing. Through genome annotation, enzymes and enzymatic pathways involved in plastic degradation which have been observed in previous studies could be identified in the isolates. The presence of known virulence factors and antibiotic-resistance genes was also confirmed via sequence analysis. Further analysis is required to determine whether the candidate genes are expressed at a higher level when plastic is provided as a sole carbon source. Deliberate inactivation of these genes to create mutants will confirm their roles in the degradation process. Additionally, these isolates may be able to survive on other plastics, an aspect yet to be explored. In the current study, biological replication was performed in triplicate (n=20), and future research with a larger sample size should be performed to understand the biodegradation capacity of *Zophobus atratus* more extensively. Furthermore, the determination of the molecular weight of plastics (before and after biodegradation) is also recommended. Overall, the plastic-degrading bacteria in the larval gut provides an excellent opportunity to develop novel approaches for plastic bioremediation. From an environmental perspective, this study marks a starting point for a systems biology approach to design more potent enzymes and bacteria to combat plastic pollution.

References

Abatenh, E., Gizaw, B., Tsegaye, Z., & Wassie, M. (2017). The Role of Microorganisms in Bioremediation- A Review. *Open Journal of Environmental Biology*, *2*(1), 038–046. https://doi.org/10.17352/ojeb.000007

Alcock, B. P., Huynh, W., Chalil, R., Smith, K. W., Raphenya, A. R., Wlodarski, M. A., Edalatmand, A., Petkau, A., Syed, S. A., Tsang, K. K., Baker, S. J. C., Dave, M., McCarthy, M. C., Mukiri, K. M., Nasir, J. A., Golbon, B., Imtiaz, H., Jiang, X., Kaur, K., … McArthur, A. G. (2023). CARD 2023: Expanded curation, support for machine learning, and resistome prediction at the Comprehensive Antibiotic Resistance Database. *Nucleic Acids Research*, *51*(D1), D690–D699. https://doi.org/10.1093/nar/gkac920

Al-Sakkaf, M. K., & Onaizi, S. A. (2023). Crude oil/water nanoemulsions stabilized by rhamnolipid biosurfactant: Effects of acidity/basicity and salinity on emulsion characteristics, stability, and demulsification. *Fuel*, *344*, 128052. https://doi.org/10.1016/j.fuel.2023.128052

Altschul, S. F., Gish, W., Miller, W., Myers, E. W., & Lipman, D. J. (1990). Basic local alignment search tool. *Journal of Molecular Biology*, *215*(3), 403–410. https://doi.org/10.1016/S0022-2836(05)80360-2

Arora, N. K. (2018). Bioremediation: A green approach for restoration of polluted ecosystems. *Environmental Sustainability*, *1*(4), 305–307. https://doi.org/10.1007/s42398-018-00036-y

Bankevich, A., Nurk, S., Antipov, D., Gurevich, A. A., Dvorkin, M., Kulikov, A. S., Lesin, V. M., Nikolenko, S. I., Pham, S., Prjibelski, A. D., Pyshkin, A. V., Sirotkin, A. V., Vyahhi, N., Tesler, G., Alekseyev, M. A., & Pevzner, P. A. (2012). SPAdes: A New

Genome Assembly Algorithm and Its Applications to Single-Cell Sequencing. *Journal of Computational Biology*, *19*(5), 455–477. https://doi.org/10.1089/cmb.2012.0021

Bardají, D. K. R., Furlan, J. P. R., & Stehling, E. G. (2019). Isolation of a polyethylene degrading Paenibacillus sp. From a landfill in Brazil. *Archives of Microbiology*, *201*(5), 699–704. https://doi.org/10.1007/s00203-019-01637-9

Bombelli, P., Howe, C. J., & Bertocchini, F. (2017). Polyethylene bio-degradation by caterpillars of the wax moth Galleria mellonella. *Current Biology*, *27*(8), R292–R293. https://doi.org/10.1016/j.cub.2017.02.060

Brandon, A. M., Gao, S.-H., Tian, R., Ning, D., Yang, S.-S., Zhou, J., Wu, W.-M., & Criddle, C. S. (2018). Biodegradation of Polyethylene and Plastic Mixtures in Mealworms (Larvae of Tenebrio molitor) and Effects on the Gut Microbiome. *Environmental Science & Technology*, *52*(11), 6526–6533. https://doi.org/10.1021/acs.est.8b02301

Brown, V. I., & Lowbury, E. J. L. (1965). Use of an improved cetrimide agar medium and other culture methods for Pseudomonas aeruginosa. *Journal of Clinical Pathology*, *18*(6), 752–756. https://doi.org/10.1136/jcp.18.6.752

Chamas, A., Moon, H., Zheng, J., Qiu, Y., Tabassum, T., Jang, J. H., Abu-Omar, M., Scott, S. L., & Suh, S. (2020). Degradation Rates of Plastics in the Environment. *ACS Sustainable Chemistry & Engineering*, *8*(9), 3494–3511. https://doi.org/10.1021/acssuschemeng.9b06635

Chatterjee, S., Chattopadhyay, P., Roy, S., & Sen, S. (2008). Bioremediation: A tool for cleaning polluted environments. *Journal of Applied Biosciences*, *11*, 594–601.

Chen, L., Yang, J., Yu, J., Yao, Z., Sun, L., Shen, Y., & Jin, Q. (2005). VFDB: A reference database for bacterial virulence factors. *Nucleic Acids Research*, *33*(Database issue), D325-328. https://doi.org/10.1093/nar/gki008

Criscuolo, A., & Gribaldo, S. (2010). BMGE (Block Mapping and Gathering with Entropy): A new software for selection of phylogenetic informative regions from multiple sequence alignments. *BMC Evolutionary Biology*, *10*(1), 210. https://doi.org/10.1186/1471-2148-10-210

Danso, D., Chow, J., & Streit, W. R. (2019). Plastics: Environmental and Biotechnological Perspectives on Microbial Degradation. *Applied and Environmental Microbiology*, *85*(19), e01095-19. https://doi.org/10.1128/AEM.01095-19

Fazito do Vale, V., Pereira, M. H., & Gontijo, N. F. (2007). Midgut pH profile and protein digestion in the larvae of Lutzomyia longipalpis (Diptera: Psychodidae). *Journal of Insect Physiology*, *53*(11), 1151–1159. https://doi.org/10.1016/j.jinsphys.2007.06.005

FTIR Micro-Spectrometer—BDD : Industrial Synchrotron Light Research Institute (Public Organization). (n.d.). Retrieved March 17, 2024, from https://www.slri.or.th/bdd/th/22-%E0B9%8C/66-ftir-micro-spectrometer.html

Fujisawa, M., Hirai, H., & Nishida, T. (2001). Degradation of Polyethylene and Nylon-66 by the Laccase-Mediator System. *Journal of Polymers and the Environment*, *9*(3), 103–108. https://doi.org/10.1023/A:1020472426516

Fursov, V. N., & Cherney, L. S. (2018). Zophobas atratus (Fabricius, 1775) – new genus and species of darkling beetles (Coleoptera, Tenebrionidae) for the fauna of Ukraine. *Ukrainian Entomological Journal*, *14*(1), Article 1. https://doi.org/10.15421/281802

Galgali, P., Varma, A. J., Puntambekar, U. S., & Gokhale, D. V. (2002). Towards biodegradable polyolefins: Strategy of anchoring minute quantities of monosaccharides and disaccharides onto functionalized polystyrene, and their effect on facilitating polymer biodegradation. *Chemical Communications*, *23*, 2884–2885. https://doi.org/10.1039/B209254A

Gambarini, V., Pantos, O., Kingsbury, J. M., Weaver, L., Handley, K. M., & Lear, G. (2022). PlasticDB: A database of microorganisms and proteins linked to plastic biodegradation. *Database*, *2022*, baac008. https://doi.org/10.1093/database/baac008

Gao, J., Ellis, L. B. M., & Wackett, L. P. (2010). The University of Minnesota Biocatalysis/Biodegradation Database: Improving public access. *Nucleic Acids Research*, *38*(suppl_1), D488–D491. https://doi.org/10.1093/nar/gkp771

Gautam, R., Bassi, A. S., & Yanful, E. K. (2007). A review of biodegradation of synthetic plastic and foams. *Applied Biochemistry and Biotechnology*, *141*(1), 85–108. https://doi.org/10.1007/s12010-007-9212-6

Goosey, M. T. (1985). Introduction to Plastics and their Important Properties for Electronic Applications. In M. T. Goosey (Ed.), *Plastics for Electronics* (pp. 1–24). Springer Netherlands. https://doi.org/10.1007/978-94-009-4942-3_1

Guindon, S., Dufayard, J.-F., Lefort, V., Anisimova, M., Hordijk, W., & Gascuel, O. (2010). New Algorithms and Methods to Estimate Maximum-Likelihood Phylogenies: Assessing the Performance of PhyML 3.0. *Systematic Biology*, *59*(3), 307–321. https://doi.org/10.1093/sysbio/syq010

Gurevich, A., Saveliev, V., Vyahhi, N., & Tesler, G. (2013). QUAST: Quality assessment tool for genome assemblies. *Bioinformatics*, *29*(8), 1072–1075. https://doi.org/10.1093/bioinformatics/btt086

Gutiérrez-Gómez, U., Servín-González, L., & Soberón-Chávez, G. (2019). Role of β-oxidation and de novo fatty acid synthesis in the production of rhamnolipids and polyhydroxyalkanoates by Pseudomonas aeruginosa. *Applied Microbiology and Biotechnology*, *103*(9), 3753–3760. https://doi.org/10.1007/s00253-019-09734-x

Hadad, D., Geresh, S., & Sivan, A. (2005). Biodegradation of polyethylene by the thermophilic bacterium Brevibacillus borstelensis. *Journal of Applied Microbiology*, *98*(5), 1093–1100. https://doi.org/10.1111/j.1365-2672.2005.02553.x

Hou, L., & Majumder, E. L.-W. (2021). Potential for and Distribution of Enzymatic Biodegradation of Polystyrene by Environmental Microorganisms. *Materials*, *14*(3), Article 3. https://doi.org/10.3390/ma14030503

Ichikawa, T., & Kurauchi, T. (2009). Larval Cannibalism and Pupal Defense Against Cannibalism in Two Species of Tenebrionid Beetles. *Zoological Science*, *26*(8), 525–529. https://doi.org/10.2108/zsj.26.525

Jabir, M. A. R., Jabir, S. A. R., & Vikineswary, S. (2012). Nutritive potential and utilization of super worm (Zophobas morio) meal in the diet of Nile tilapia (Oreochromis niloticus) juvenile. *African Journal of Biotechnology*, *11*(24), Article 24. https://doi.org/10.4314/ajb.v11i24

Jeon, H. J., & Kim, M. N. (2015). Functional analysis of alkane hydroxylase system derived from Pseudomonas aeruginosa E7 for low molecular weight polyethylene biodegradation. *International Biodeterioration & Biodegradation*, *103*, 141–146. https://doi.org/10.1016/j.ibiod.2015.04.024

Jolley, K. A., Bray, J. E., & Maiden, M. C. J. (2018). Open-access bacterial population genomics: BIGSdb software, the PubMLST.org website and their applications. *Wellcome Open Research*, *3*, 124. https://doi.org/10.12688/wellcomeopenres.14826.1

Junier, T., & Zdobnov, E. M. (2010). The Newick utilities: High-throughput phylogenetic tree processing in the Unix shell. *Bioinformatics*, *26*(13), 1669–1670. https://doi.org/10.1093/bioinformatics/btq243

Juwarkar, A. A., Singh, S. K., & Mudhoo, A. (2010). A comprehensive overview of elements in bioremediation. *Reviews in Environmental Science and Bio/Technology*, *9*(3), 215–288. https://doi.org/10.1007/s11157-010-9215-6

Kanehisa, M., Sato, Y., & Morishima, K. (2016). BlastKOALA and GhostKOALA: KEGG Tools for Functional Characterization of Genome and Metagenome Sequences. *Journal of Molecular Biology*, *428*(4), 726–731. https://doi.org/10.1016/j.jmb.2015.11.006

Katoh, K., & Standley, D. M. (2013). MAFFT Multiple Sequence Alignment Software Version 7: Improvements in Performance and Usability. *Molecular Biology and Evolution*, *30*(4), 772–780. https://doi.org/10.1093/molbev/mst010

Khandare, S. D., Chaudhary, D. R., & Jha, B. (2021). Marine bacterial biodegradation of low-density polyethylene (LDPE) plastic. *Biodegradation*, *32*(2), 127–143. https://doi.org/10.1007/s10532-021-09927-0

Kiel, G. R., Lundberg, D. J., Prince, E., Husted, K. E. L., Johnson, A. M., Lensch, V., Li, S., Shieh, P., & Johnson, J. A. (2022). Cleavable Comonomers for Chemically Recyclable Polystyrene: A General Approach to Vinyl Polymer Circularity. *Journal of the American Chemical Society*, *144*(28), 12979–12988. https://doi.org/10.1021/jacs.2c05374

Kim, H. R., Lee, H. M., Yu, H. C., Jeon, E., Lee, S., Li, J., & Kim, D.-H. (2020). Biodegradation of Polystyrene by Pseudomonas sp. Isolated from the Gut of Superworms (Larvae of Zophobas atratus). *Environmental Science & Technology*, *54*(11), 6987–6996. https://doi.org/10.1021/acs.est.0c01495

Kim, H.-W., Jo, J. H., Kim, Y.-B., Le, T.-K., Cho, C.-W., Yun, C.-H., Chi, W. S., & Yeom, S.-J. (2021a). Biodegradation of polystyrene by bacteria from the soil in common environments. *Journal of Hazardous Materials*, *416*, 126239. https://doi.org/10.1016/j.jhazmat.2021.126239

Kim, H.-W., Jo, J. H., Kim, Y.-B., Le, T.-K., Cho, C.-W., Yun, C.-H., Chi, W. S., & Yeom, S.-J. (2021b). Biodegradation of polystyrene by bacteria from the soil in common environments. *Journal of Hazardous Materials*, *416*, 126239. https://doi.org/10.1016/j.jhazmat.2021.126239

Kyaw, B. M., Champakalakshmi, R., Sakharkar, M. K., Lim, C. S., & Sakharkar, K. R. (2012). Biodegradation of Low Density Polythene (LDPE) by Pseudomonas Species. *Indian Journal of Microbiology*, *52*(3), 411–419. https://doi.org/10.1007/s12088-012-0250-6

LaMar, D. (2015). *FastQC*. https://qubeshub.org/resources/fastqc

Landrock, A. H. (1995). *Handbook of Plastic Foams: Types, Properties, Manufacture and Applications*. Elsevier.

Lee, D. G., Urbach, J. M., Wu, G., Liberati, N. T., Feinbaum, R. L., Miyata, S., Diggins, L. T., He, J., Saucier, M., Déziel, E., Friedman, L., Li, L., Grills, G., Montgomery, K., Kucherlapati, R., Rahme, L. G., & Ausubel, F. M. (2006). Genomic analysis reveals that Pseudomonas aeruginosa virulence is combinatorial. *Genome Biology*, *7*(10), R90. https://doi.org/10.1186/gb-2006-7-10-r90

Lee, H. M., Kim, H. R., Jeon, E., Yu, H. C., Lee, S., Li, J., & Kim, D.-H. (2020). Evaluation of the Biodegradation Efficiency of Four Various Types of Plastics by Pseudomonas aeruginosa Isolated from the Gut Extract of Superworms. *Microorganisms*, *8*(9), Article 9. https://doi.org/10.3390/microorganisms8091341

Lefort, V., Longueville, J.-E., & Gascuel, O. (2017). SMS: Smart Model Selection in PhyML. *Molecular Biology and Evolution*, *34*(9), 2422–2424. https://doi.org/10.1093/molbev/msx149

Lemoine, F., Correia, D., Lefort, V., Doppelt-Azeroual, O., Mareuil, F., Cohen-Boulakia, S., & Gascuel, O. (2019). NGPhylogeny.fr: New generation phylogenetic services for non-

specialists. *Nucleic Acids Research*, *47*(W1), W260–W265. https://doi.org/10.1093/nar/gkz303

Lemoine, F., Domelevo Entfellner, J.-B., Wilkinson, E., Correia, D., Dávila Felipe, M., De Oliveira, T., & Gascuel, O. (2018). Renewing Felsenstein's phylogenetic bootstrap in the era of big data. *Nature*, *556*(7702), Article 7702. https://doi.org/10.1038/s41586-018-0043-0

Letunic, I., & Bork, P. (2021). Interactive Tree Of Life (iTOL) v5: An online tool for phylogenetic tree display and annotation. *Nucleic Acids Research*, *49*(W1), W293–W296. https://doi.org/10.1093/nar/gkab301

Lou, Y., Ekaterina, P., Yang, S.-S., Lu, B., Liu, B., Ren, N., Corvini, P. F.-X., & Xing, D. (2020). Biodegradation of Polyethylene and Polystyrene by Greater Wax Moth Larvae (Galleria mellonella L.) and the Effect of Co-diet Supplementation on the Core Gut Microbiome. *Environmental Science & Technology*, *54*(5), 2821–2831. https://doi.org/10.1021/acs.est.9b07044

Luo, L., Wang, Y., Guo, H., Yang, Y., Qi, N., Zhao, X., Gao, S., & Zhou, A. (2021). Biodegradation of foam plastics by Zophobas atratus larvae (Coleoptera: Tenebrionidae) associated with changes of gut digestive enzymes activities and microbiome. *Chemosphere*, *282*, 131006. https://doi.org/10.1016/j.chemosphere.2021.131006

Mohee, R., & Unmar, G. (2007). Determining biodegradability of plastic materials under controlled and natural composting environments. *Waste Management*, *27*(11), 1486–1493. https://doi.org/10.1016/j.wasman.2006.07.023

Mukherjee, S., & Kundu, P. P. (2014). Alkaline fungal degradation of oxidized polyethylene in black liquor: Studies on the effect of lignin peroxidases and manganese peroxidases. *Journal of Applied Polymer Science*, *131*(17). https://doi.org/10.1002/app.40738

Nowak, B., Pająk, J., Drozd-Bratkowicz, M., & Rymarz, G. (2011). Microorganisms participating in the biodegradation of modified polyethylene films in different soils under laboratory conditions. *International Biodeterioration & Biodegradation*, *65*(6), 757–767. https://doi.org/10.1016/j.ibiod.2011.04.007

Oliveira, J., Belchior, A., da Silva, V. D., Rotter, A., Petrovski, Ž., Almeida, P. L., Lourenço, N. D., & Gaudêncio, S. P. (2020). Marine Environmental Plastic Pollution: Mitigation by Microorganism Degradation and Recycling Valorization. *Frontiers in Marine Science*, *7*. https://doi.org/10.3389/fmars.2020.567126

Omokhagbor Adams, G., Tawari Fufeyin, P., Eruke Okoro, S., & Ehinomen, I. (2020). Bioremediation, Biostimulation and Bioaugmention: A Review. *International Journal of Environmental Bioremediation & Biodegradation*, *3*(1), 28–39. https://doi.org/10.12691/ijebb-3-1-5

(Orr), I. G., Hadar, Y., & Sivan, A. (2004). Colonization, biofilm formation and biodegradation of polyethylene by a strain of Rhodococcus ruber. *Applied Microbiology and Biotechnology*, *65*(1), 97–104. https://doi.org/10.1007/s00253-004-1584-8

Page, A. J., Cummins, C. A., Hunt, M., Wong, V. K., Reuter, S., Holden, M. T. G., Fookes, M., Falush, D., Keane, J. A., & Parkhill, J. (2015). Roary: Rapid large-scale prokaryote pan genome analysis. *Bioinformatics (Oxford, England)*, *31*(22), 3691–3693. https://doi.org/10.1093/bioinformatics/btv421

Park, H. C., Jung, B. H., Han, T., Lee, Y. B., Kim, S.-H., & Kim, N. J. (2013). Taxonomy of introduced commercial insect, Zophobas atratus (Coleoptera: Tenebrionidae) and a comparison of DNA barcoding with similar tenebrionids, Promethis valgipes and Tenebrio molitor in Korea. *Journal of Sericultural and Entomological Science*, *51*(2), 185–190. https://doi.org/10.7852/jses.2013.51.2.185

Parks, D. H., Imelfort, M., Skennerton, C. T., Hugenholtz, P., & Tyson, G. W. (2015). CheckM: Assessing the quality of microbial genomes recovered from isolates, single cells, and metagenomes. *Genome Research*, *25*(7), 1043–1055. https://doi.org/10.1101/gr.186072.114

Paysan-Lafosse, T., Blum, M., Chuguransky, S., Grego, T., Pinto, B. L., Salazar, G. A., Bileschi, M. L., Bork, P., Bridge, A., Colwell, L., Gough, J., Haft, D. H., Letunić, I., Marchler-Bauer, A., Mi, H., Natale, D. A., Orengo, C. A., Pandurangan, A. P., Rivoire, C., … Bateman, A. (2023). InterPro in 2022. *Nucleic Acids Research*, *51*(D1), D418–D427. https://doi.org/10.1093/nar/gkac993

Peng, B.-Y., Li, Y., Fan, R., Chen, Z., Chen, J., Brandon, A. M., Criddle, C. S., Zhang, Y., & Wu, W.-M. (2020). Biodegradation of low-density polyethylene and polystyrene in superworms, larvae of Zophobas atratus (Coleoptera: Tenebrionidae): Broad and limited extent depolymerization. *Environmental Pollution*, *266*, 115206. https://doi.org/10.1016/j.envpol.2020.115206

Peng, B.-Y., Su, Y., Chen, Z., Chen, J., Zhou, X., Benbow, M. E., Criddle, C. S., Wu, W.-M., & Zhang, Y. (2019). Biodegradation of Polystyrene by Dark (Tenebrio obscurus) and Yellow (Tenebrio molitor) Mealworms (Coleoptera: Tenebrionidae). *Environmental Science & Technology*, *53*(9), 5256–5265. https://doi.org/10.1021/acs.est.8b06963

Rajandas, H., Parimannan, S., Sathasivam, K., Ravichandran, M., & Su Yin, L. (2012). A novel FTIR-ATR spectroscopy based technique for the estimation of low-density polyethylene biodegradation. *Polymer Testing*, *31*(8), 1094–1099. https://doi.org/10.1016/j.polymertesting.2012.07.015

Ramos-Elorduy, J. (2009). Anthropo-entomophagy: Cultures, evolution and sustainability. *Entomological Research*, *39*(5), 271–288. https://doi.org/10.1111/j.1748-5967.2009.00238.x

Robertson, J., & Nash, J. H. E. (2018). MOB-suite: Software tools for clustering, reconstruction and typing of plasmids from draft assemblies. *Microbial Genomics*, *4*(8), e000206. https://doi.org/10.1099/mgen.0.000206

Rumbos, C. I., & Athanassiou, C. G. (2021). The Superworm, Zophobas morio (Coleoptera:Tenebrionidae): A 'Sleeping Giant' in Nutrient Sources. *Journal of Insect Science*, *21*(2), 13. https://doi.org/10.1093/jisesa/ieab014

Sanluis-Verdes, A., Colomer-Vidal, P., Rodriguez-Ventura, F., Bello-Villarino, M., Spinola-Amilibia, M., Ruiz-Lopez, E., Illanes-Vicioso, R., Castroviejo, P., Aiese Cigliano, R., Montoya, M., Falabella, P., Pesquera, C., Gonzalez-Legarreta, L., Arias-Palomo, E., Solà, M., Torroba, T., Arias, C. F., & Bertocchini, F. (2022). Wax worm saliva and the enzymes therein are the key to polyethylene degradation by Galleria mellonella. *Nature Communications*, *13*(1), Article 1. https://doi.org/10.1038/s41467-022-33127-w

Santo, M., Weitsman, R., & Sivan, A. (2013). The role of the copper-binding enzyme – laccase – in the biodegradation of polyethylene by the actinomycete Rhodococcus ruber. *International Biodeterioration & Biodegradation*, *84*, 204–210. https://doi.org/10.1016/j.ibiod.2012.03.001

Scanning Electron Microscope—Environmental Health and Safety—Purdue University. (n.d.). Retrieved March 17, 2024, from https://www.purdue.edu/ehps/rem/laboratory/equipment%20safety/Research%20Equipment/sem.html

Schwarz, A. E., Lensen, S. M. C., Langeveld, E., Parker, L. A., & Urbanus, J. H. (2023). Plastics in the global environment assessed through material flow analysis, degradation and environmental transportation. *Science of The Total Environment*, *875*, 162644. https://doi.org/10.1016/j.scitotenv.2023.162644

Seemann, T. (2014). Prokka: Rapid prokaryotic genome annotation. *Bioinformatics (Oxford, England)*, *30*(14), 2068–2069. https://doi.org/10.1093/bioinformatics/btu153

Shabbir, S., Faheem, M., Ali, N., Kerr, P. G., Wang, L.-F., Kuppusamy, S., & Li, Y. (2020). Periphytic biofilm: An innovative approach for biodegradation of microplastics. *Science of The Total Environment*, *717*, 137064. https://doi.org/10.1016/j.scitotenv.2020.137064

Shah, A. A., Hasan, F., Hameed, A., & Ahmed, S. (2008). Biological degradation of plastics: A comprehensive review. *Biotechnology Advances*, *26*(3), 246–265. https://doi.org/10.1016/j.biotechadv.2007.12.005

Soares Araújo, R. R., dos Santos Benfica, T. A. R., Ferraz, V. P., & Moreira Santos, E. (2019). Nutritional composition of insects *Gryllus assimilis* and *Zophobas morio*: Potential foods harvested in Brazil. *Journal of Food Composition and Analysis*, *76*, 22–26. https://doi.org/10.1016/j.jfca.2018.11.005

Spilker, T., Coenye, T., Vandamme, P., & LiPuma, J. J. (2004). PCR-Based Assay for Differentiation of Pseudomonas aeruginosa from Other Pseudomonas Species Recovered from Cystic Fibrosis Patients. *Journal of Clinical Microbiology*, *42*(5), 2074–2079. https://doi.org/10.1128/JCM.42.5.2074-2079.2004

Sun, J., Prabhu, A., Aroney, S. T. N., & Rinke, C. (2022). Insights into plastic biodegradation: Community composition and functional capabilities of the superworm (Zophobas morio) microbiome in styrofoam feeding trials. *Microbial Genomics*, *8*(6), mgen000842. https://doi.org/10.1099/mgen.0.000842

Taboada, B., Estrada, K., Ciria, R., & Merino, E. (2018). Operon-mapper: A web server for precise operon identification in bacterial and archaeal genomes. *Bioinformatics*, *34*(23), 4118–4120. https://doi.org/10.1093/bioinformatics/bty496

Taghavi, N., Singhal, N., Zhuang, W.-Q., & Baroutian, S. (2021). Degradation of plastic waste using stimulated and naturally occurring microbial strains. *Chemosphere*, *263*, 127975. https://doi.org/10.1016/j.chemosphere.2020.127975

Toribio, J., Escalante, A. E., & Soberón-Chávez, G. (2010). Rhamnolipids: Production in bacteria other than Pseudomonas aeruginosa. *European Journal of Lipid Science and Technology*, *112*(10), 1082–1087. https://doi.org/10.1002/ejlt.200900256

Tribedi, P., & Sil, A. K. (2013). Low-density polyethylene degradation by Pseudomonas sp. AKS2 biofilm. *Environmental Science and Pollution Research*, *20*(6), 4146–4153. https://doi.org/10.1007/s11356-012-1378-y

Tschinkel, W. R. (1984). Zophobas atratus (Fab.) and Z. rugipes Kirsch (Coleoptera: Tenebrionidae) Are the Same Species. *The Coleopterists Bulletin*, *38*(4), 325–333.

Vidali, M. (2001). Bioremediation. An overview. *Pure and Applied Chemistry*, *73*(7), 1163–1172. https://doi.org/10.1351/pac200173071163

Wang, Z., Xin, X., Shi, X., & Zhang, Y. (2020). A polystyrene-degrading Acinetobacter bacterium isolated from the larvae of Tribolium castaneum. *Science of The Total Environment*, *726*, 138564. https://doi.org/10.1016/j.scitotenv.2020.138564

Wasi, S., Tabrez, S., & Ahmad, M. (2013). Use of Pseudomonas spp. for the bioremediation of environmental pollutants: A review. *Environmental Monitoring and Assessment*, *185*(10), 8147–8155. https://doi.org/10.1007/s10661-013-3163-x

Wei, Z., Wang, J. J., Gaston, L. A., Li, J., Fultz, L. M., DeLaune, R. D., & Dodla, S. K. (2020). Remediation of crude oil-contaminated coastal marsh soil: Integrated effect of biochar, rhamnolipid biosurfactant and nitrogen application. *Journal of Hazardous Materials*, *396*, 122595. https://doi.org/10.1016/j.jhazmat.2020.122595

Wilkes, R. A., & Aristilde, L. (2017). Degradation and metabolism of synthetic plastics and associated products by Pseudomonas sp.: Capabilities and challenges. *Journal of Applied Microbiology*, *123*(3), 582–593. https://doi.org/10.1111/jam.13472

Wright, S. L., Gouin, T., Koelmans, A. A., & Scheuermann, L. (2021). Development of screening criteria for microplastic particles in air and atmospheric deposition: Critical review and applicability towards assessing human exposure. *Microplastics and Nanoplastics*, *1*(1), 6. https://doi.org/10.1186/s43591-021-00006-y

Yan, P., Lu, M., Yang, Q., Zhang, H.-L., Zhang, Z.-Z., & Chen, R. (2012). Oil recovery from refinery oily sludge using a rhamnolipid biosurfactant-producing Pseudomonas. *Bioresource Technology*, *116*, 24–28. https://doi.org/10.1016/j.biortech.2012.04.024

Yang, S.-S., Ding, M.-Q., He, L., Zhang, C.-H., Li, Q.-X., Xing, D.-F., Cao, G.-L., Zhao, L., Ding, J., Ren, N.-Q., & Wu, W.-M. (2021). Biodegradation of polypropylene by yellow mealworms (Tenebrio molitor) and superworms (Zophobas atratus) via gut-microbe-dependent depolymerization. *Science of The Total Environment*, *756*, 144087. https://doi.org/10.1016/j.scitotenv.2020.144087

Yang, S.-S., Ding, M.-Q., Zhang, Z.-R., Ding, J., Bai, S.-W., Cao, G.-L., Zhao, L., Pang, J.-W., Xing, D.-F., Ren, N.-Q., & Wu, W.-M. (2021). Confirmation of biodegradation of low-density polyethylene in dark- versus yellow- mealworms (larvae of Tenebrio obscurus versus Tenebrio molitor) via. Gut microbe-independent depolymerization. *Science of The Total Environment*, *789*, 147915. https://doi.org/10.1016/j.scitotenv.2021.147915

Yang, Y., Wang, J., & Xia, M. (2020). Biodegradation and mineralization of polystyrene by plastic-eating superworms Zophobas atratus. *Science of The Total Environment*, *708*, 135233. https://doi.org/10.1016/j.scitotenv.2019.135233

Yang, Y., Yang, J., Wu, W.-M., Zhao, J., Song, Y., Gao, L., Yang, R., & Jiang, L. (2015a). Biodegradation and Mineralization of Polystyrene by Plastic-Eating Mealworms: Part 1. Chemical and Physical Characterization and Isotopic Tests. *Environmental Science & Technology*, *49*(20), 12080–12086. https://doi.org/10.1021/acs.est.5b02661

Yang, Y., Yang, J., Wu, W.-M., Zhao, J., Song, Y., Gao, L., Yang, R., & Jiang, L. (2015b). Biodegradation and Mineralization of Polystyrene by Plastic-Eating Mealworms: Part 2. Role of Gut Microorganisms. *Environmental Science & Technology*, *49*(20), 12087–12093. https://doi.org/10.1021/acs.est.5b02663

Yeom, S.-J., Le, T.-K., & Yun, C.-H. (2022). P450-driven plastic-degrading synthetic bacteria. *Trends in Biotechnology*, *40*(2), 166–179. https://doi.org/10.1016/j.tibtech.2021.06.003

Zaman, I., Turjya, R. R., Shakil, M. S., Al Shahariar, M., Md. Rezanur Rahman, H. E., Ahmed, A., & Hossain, M. M. (2024). Biodegradation of polyethylene and polystyrene by Zophobas atratus larvae from Bangladeshi source and isolation of two plastic-degrading gut bacteria. *Environmental Pollution*, 123446. https://doi.org/10.1016/j.envpol.2024.123446

Zeenat, Elahi, A., Bukhari, D. A., Shamim, S., & Rehman, A. (2021). Plastics degradation by microbes: A sustainable approach. *Journal of King Saud University - Science*, *33*(6), 101538. https://doi.org/10.1016/j.jksus.2021.101538

Zielińska, E., Zieliński, D., Jakubczyk, A., Karaś, M., Pankiewicz, U., Flasz, B., Dziewięcka, M., & Lewicki, S. (2021). The impact of polystyrene consumption by edible insects Tenebrio molitor and Zophobas morio on their nutritional value, cytotoxicity, and oxidative stress parameters. *Food Chemistry*, *345*, 128846. https://doi.org/10.1016/j.foodchem.2020.128846

Appendix A

This study has been published in the Journal “Environmental Pollution”. (2022 Journal Impact factor 8.9 with CiteScore 14.9)

(Zaman et al., 2024)

Zaman, I., Turjya, R. R., Shakil, M. S., Al Shahariar, M., Md. Rezanur Rahman, H. E., Ahmed, A., & Hossain, M. M. (2024). Biodegradation of polyethylene and polystyrene by Zophobas atratus larvae from Bangladeshi source and isolation of two plastic-degrading gut bacteria. *Environmental Pollution*, 123446. https://doi.org/10.1016/j.envpol.2024.123446